Seasonal Persistence and Propagation of Intraseasonal Patterns over the Indian Monsoon Region

V. Krishnamurthy and J. Shukla

Center for Ocean-Land-Atmosphere Studies
Institute of Global Environment and Society, Inc.
Calverton, Maryland
and
School of Computational Sciences
George Mason University
Fairfax, Virginia

February 2006

Corresponding author's address:

V. Krishnamurthy
COLA, IGES
4041 Powder Mill Road, Suite 302
Calverton, MD 20705, USA

E-mail: krishna@cola.iges.org

Abstract

The space-time evolution of convection over the monsoon region containing the Indian subcontinent, the Indian Ocean and the West Pacific has been studied. A multi-channel singular spectrum analysis of the daily outgoing longwave radiation has yielded two intraseasonal oscillatory patterns and two large-scale standing patterns as the most dominant modes of intraseasonal variability. The oscillatory modes vary on time scales of about 45 and 28 days and their average cycles of variability are shown to correspond to the life cycles of active and break periods of monsoon rainfall over India. During an active (break) cycle, a convection (dry) anomaly zone first appears in the equatorial Indian Ocean, subsequently expands to cover the Indian subcontinent and finally contracts to disappear in the northern part of India. Some eastward and northward movements are found to be associated with both oscillatory modes, while westward movement may also be associated with the 28-day mode. The oscillatory modes are shown to have a large spatial scale extending to the West Pacific.

One of the standing modes has anomalies of uniform sign covering the entire region and is related to El Niño and Southern Oscillation (ENSO) pattern. The other standing mode has a dipole structure in the equatorial Indian Ocean associated with large-scale anomalies over India with the same sign as those over the western part of the dipole. These two standing modes persist throughout the monsoon season, each maintaining its respective pattern. The seasonal mean monsoon is mainly determined by the two standing patterns, without much contribution from the oscillatory modes. The relative role of the standing patterns (ENSO mode and dipole mode) seems to be important in determining the seasonal mean during certain years.

1. Introduction

The statistical forecasts of seasonal mean rainfall over India issued by the India Meteorological Department since 1924 use regional and global climate parameters as predictors (Thapliyal 1990, Rajeevan 2001), and their origin goes back to Walker's discovery of correlation of the Indian rainfall with variables observed at various global locations. The potential for long-term prediction by dynamical models was recognized from general circulation model (GCM) results which indicated that a large part of the monsoon variability is determined by slowly varying boundary conditions such as the sea surface temperature (SST), soil moisture and snow cover (Charney and Shukla 1981). A proper understanding of the response due to slowly varying components of the system and the relative role of the intraseasonal fluctuations of the monsoon is essential for successful prediction of the seasonal mean monsoon.

The intraseasonal variability of the monsoon is manifested as active periods of high rainfall and break periods with weak or no rainfall during June-July-August-September (JJAS) (see reviews by Webster et al. 1998; Krishnamurthy and Kinter, 2002). The temporal character of the active and break phases is described in terms of intraseasonal "oscillations" with time scales that broadly fall into 30-60 day and 10-20 day range in studies involving spectral analysis of monsoon variables. Spectral peaks in the range 10-20 days were found in pressure, cloud cover and static stability over India for one to three seasons (Krishnamurti and Bhalme 1976) while a longer data set of surface pressure indicated 10-20 day, 20-30 day and 30-40 day variability (Krishnamurti and Ardanuy 1980). An analysis of a long data set of daily rainfall over India showed a 40-50 day spectral peak (Hartmann and Michelsen 1989). Both 10-20 day and 40-50 day periods were also found in convection data (Yasunari 1979).

The main spatial feature of the intraseasonal monsoon variability is described by the movement of the monsoon trough that exists over India during the northern summer. The active periods occur when the monsoon trough is over central India whereas the break periods are established when the trough has moved north reaching the foothills of the Himalayas (e.g., Ramamurthy 1969). Consistent with this picture, Krishnamurthy and Shukla (2000) used 70-year long high resolution daily rainfall data to show that the dominant mode of the active phase of the intraseasonal monsoon rainfall variability consisted of above-normal rainfall over central India and the Western Ghats and below-normal rainfall over northern India in the sub-Himalayan region and over southeastern India. The pattern is reversed with anomalies of opposite sign during the break phase. However, the dominant mode of the seasonal mean rainfall was shown to be a large-scale pattern with anomalies of one sign over entire India persisting for the entire season. The relative strength of the intraseasonal modes and the seasonally persisting modes becomes important in determining the success in predicting the seasonal mean monsoon rainfall.

However, there was a lack of proper description of the space-time structure of the intraseasonal "oscillations" of the monsoon rainfall. As a step toward understanding whether the intraseasonal variations arise from some internal instability, as yet an unsolved problem, it is necessary to know if the oscillations at different time scales are distinct and what relation they have with the active and break phases. Further, for success in predicting seasonal mean monsoon rainfall, it is also necessary to find the relative contribution of these intraseasonal oscillations to the seasonal mean and to find if there are seasonally persisting components that mostly determine the seasonal mean rainfall as suggested earlier (Charney and Shukla 1981 and Krishnamurthy and Shukla 2000).

A recent study (Krishnamurthy and Shukla 2005) has provided such a detailed description showing that there are two distinct intraseasonal modes and three distinct seasonally persisting components in the rainfall over India. These spatio-temporal patterns emerge as distinct eigenmodes of multi-channel singular spectrum analysis (MSSA) of a 70-year long daily Indian rainfall data record that was not subject to any kind of band-pass pre-filtering. The two nonperiodic oscillatory modes have average periods centered at 45 and 20 days, and describe the development, maturation and demise of active and break phases during each cycle. The 45-day mode showed northeastward propagation whereas the 20-day showed northwestward propagation. The seasonal mean rainfall is mostly determined by the eigenmodes with standing patterns that persist with anomalies of same sign throughout most of the season.

The intraseasonal variability of the Indian rainfall has been described in terms of northward propagation of convection from the central equatorial Indian Ocean to the Indian subcontinent (e.g., Sikka and Gadgil 1980). It has also been suggested that the northward propagation is accompanied by eastward propagation over the equatorial Indian Ocean (e.g., Lau and Chan 1986 and Wang and Rui 1990). While these studies emphasize the importance of northward propagation, Lawrence and Webster (2001) argue that the eastward propagation of convection is always related to the northward movement and is fundamental to the variability over both the Indian Ocean and the Indian continent. They propose that the summer intraseasonal variability should be thought of as wintertime variability (i.e., Madden-Julian Oscillation) modified by a basic state. Independent northward moving intraseasonal oscillations due to internal dynamical mechanisms are also shown to exist in atmospheric GCM (AGCM) simulations (Jiang et al. 2004). In addition to the eastward propagation, weak westward movement of convection toward the Indian continent has also been noted (Krishnamurti and

Ardanuy 1980, Wang and Rui 1990, and Annamalai and Slingo 2001). Although various studies have associated the movements of convection zones over to the Indian continent with the active and break phases of monsoon (e.g., Krishnan et al. 2000, Lawrence and Webster 2002, Annamalai and Slingo 2001, and Annamalai and Sperber 2005), the direct relation with the rainfall over India is missing. The association of propagation of convection with the intraseasonal oscillations with periods such as 30-60 day and 10-20 day is based on data pre-filtered to be in the desired frequency band (e.g., Lau and Chan 1986, Annamalai and Slingo 2001, and Lawrence and Webster 2002).

Research to date has not addressed the question of whether there are daily patterns in monsoon variables that reveal a seasonally persisting signature as a possible response to the influence of boundary forcings over the larger monsoon region that includes the Indian Ocean. An analysis of band pass filtered latent heat flux from reanalysis data has indicated that air-sea interaction over the Indian Ocean plays an important role in the development of intraseasonal oscillations and their associated northward and eastward propagation (Kemball-Cook and Wang 2001). Hybrid coupled model experiments have shown strong coupling between intraseasonal oscillations and SST in the Indian Ocean (Fu et al. 2003 and Fu and Wang 2004). However, the intraseasonal oscillation in observed outgoing longwave radiation (OLR) has been shown to be uncorrelated with the seasonal SST anomalies (Lawrence and Webster 2001).

The need for a better understanding of the coherent space-time structure of the intraseasonal variability of monsoon over the larger region consisting of the Indian subcontinent and the Indian Ocean is the motivation for this study. The main aim is to obtain a more precise space-time character of the intraseasonal "oscillations" occurring over the larger monsoon region at different time scales and to find large-scale patterns that persist with seasonal signature. The

relative strengths of these different modes in determining the seasonal mean monsoon rainfall are also investigated. The objectives of this paper are achieved by analyzing daily OLR data over the Indian subcontinent and oceanic region containing the Indian Ocean and the West Pacific. The convection data are used because of the unavailability of reliable daily rainfall data for this larger region. The method of analysis is similar to that used in the earlier study of rainfall over just the land points over India (Krishnamurthy and Shukla 2005). However, the results of this paper go beyond the earlier study by determining the evolution of the intraseasonal oscillations, their propagation characteristics over the oceanic region and the Indian subcontinent and establishing the relation to the active and break phases of the Indian monsoon. By extending the analysis to a larger region that includes the Indian Ocean and the West Pacific, it is expected that the results revealed in the patterns of convection involve the influences of the oceanic boundary forcing. By performing MSSA of OLR over the larger monsoon region, a more precise description of two distinct propagating intraseasonal modes related to the active and break phases of the monsoon is obtained. It will be shown that the propagation of these modes simply corresponds to expansion of convection anomaly zones during certain important phases of the oscillation. Another significant result shows that there are two distinct large-scale standing patterns, one with the El Niño and Southern Oscillation (ENSO) signature and other with a dipole structure, that are the main contributors to the seasonal mean Indian rainfall with implication on the relative roles of the Indian and Pacific Oceans.

The data and methods of analysis are described in section 2. In section 3, the life cycles of convection corresponding to the active and break phases are shown. The results of MSSA of OLR over the larger monsoon region are discussed in section 4. Summary and conclusions are given in section 5.

2. Data and method of analysis

a. Data

To analyze the deep convection over the larger monsoon region, the outgoing longwave radiation data from the National Oceanic and Atmospheric Administration (NOAA) are used in this study. The daily averages of OLR on a 2.5° longitude × 2.5° latitude grid for the period 1975-2002 are analyzed. The study excludes 1978 when the data were unavailable due to problems with the satellite. The OLR dataset also serves as a proxy for precipitation, especially over the oceanic region. Because of questionable reliability, daily reanalysis precipitation data were not considered.

To relate the analysis of convection to rainfall over India, two gridded datasets of daily rainfall over land points in India are used. The first dataset is based on observations at 365 rain gauge stations in India for the period 1975-1989, and originated from the study of Singh et al. (1992). These data were regridded on to a 1.25° longitude × 1.25° latitude grid at the Center for Ocean-Land-Atmosphere Studies (M. Fennessy, personal communication). The second rainfall dataset is the gauge-based analyses of daily precipitation over global land areas (version 0103) created at the Climate Prediction Center (CPC) of NOAA and available as part of the International Satellite and Land Surface Climatology Project (ISLSCP) Initiative II data collection. This data set contains daily mean precipitation on a 1° longitude × 1° latitude grid for the period 1986-2002. Monthly mean SST data (HadISST 1.1 version) from the Hadley Centre for Climate Prediction and Research have also been used.

The daily climatology of each data set was calculated as the mean (for the length of the data set) of the total daily values for each calendar day. The daily anomalies are obtained by subtracting the climatology from the total field. The JJAS seasonal anomalies are the averages

of the daily values over 1 June to 30 September. For a coherent analysis without the presence of very high frequency fluctuations, the daily data were converted to 5-day running means.

b. Multi-channel singular spectrum analysis

Multi-channel singular spectrum analysis (MSSA) is used to obtain distinct intraseasonal space-time patterns of convection over the larger monsoon region that includes the Indian Ocean. This method is useful to extract space-time structure of oscillatory modes and persisting modes and has been applied to study the intraseasonal variability (Plaut and Vautard 1994; Krishnamurthy and Shukla 2005). A review by Ghil et al. (2002) describes the mathematical formulation and the technique in detail.

In this study, the MSSA is applied to daily OLR anomalies following exactly the same procedure used for daily Indian rainfall anomalies by Krishnamurthy and Shukla (2005). MSSA is applied to data consisting of time series of L channels (or grid points) specified at N discrete times. The lag-covariance matrix of the multi-channel time series at temporal lags from 0 to $M-1$ is diagonalized to obtain LM eigenvalues and LM eigenvectors. Each eigenvector, called the space-time empirical orthogonal function (ST-EOF), consists of M sequence of maps. The corresponding space-time principal component (ST-PC), of time length $N' = N - M + 1$, is the projection coefficient of the data onto the ST-EOF, and the eigenvalues determine the variance.

The part of the original time series corresponding to a particular eigenmode is the reconstructed component (RC), and is constructed from the original data using the corresponding ST-EOF and ST-PC (see e.g., Ghil et al. 2002). The RCs are maps on the same grid (or multi-channel) as the original field, and their time length and sequence are exactly those of the original time series. For a pair of eigenmodes identified as oscillatory, the amplitude $A(t)$ and the phase

angle $\theta(t)$ are determined from the corresponding RC. The RCs of non-oscillatory modes are examined for persisting behavior.

c. Space-time frequency spectrum

To obtain additional information on the propagation characteristics of the RCs, space-time spectral analysis is used. This method is useful to identify the spatial scales and the periods associated with propagating modes and also to identify the standing patterns. The usefulness of this method in intraseasonal studies has been demonstrated in earlier by Wheeler and Kiladis (1999) who also provide technical details. Since MSSA provides detailed information about the space-time evolution, the wavenumber-frequency analysis is used for support evidence and to remove misinterpretation regarding the propagation characteristics. The spectral analysis is applied separately to suitably averaged data in meridional and zonal extents. In this study, when the space-time domain of the RC is transformed into wavenumber-frequency domain, the wavenumbers refer to the meridional and zonal extent of the limited domain of the monsoon region over the Indian Ocean and the Indian subcontinent. Fast Fourier transforms (FFTs) of the discrete data in space and time are used to compute the spectra.

3. Active and break monsoon phases

The spatial structure of the OLR anomalies over the Indian Ocean and the Indian subcontinent during active and break phases of the Indian monsoon rainfall is described in this section. The active and break periods identified in this study are based on the daily rainfall anomalies averaged over the land points in India. This area averaged rainfall will be referred to as the Indian monsoon rainfall (IMR) index. The active (break) phase is defined as the period

when the daily anomaly IMR index is above (below) a threshold of one-half of the standard deviation of the IMR index for at least five consecutive days. This definition is similar to that of Krishnamurthy and Shukla (2000) who used the principal component of the dominant mode of the daily rainfall instead of the IMR index. Both definitions are found to identify almost the same active and break days. Using the daily rainfall data described in section 2, the active and break periods were identified for the period 1975-2002.

a. Composites of OLR anomalies

The daily OLR anomalies were averaged separately over all active and break days during JJAS 1975-2002 to construct the active and break composites. The composites are shown in Fig. 1a for the region (40°E–100°E, 20°S–35°N). The active composite has strong convection over India and the adjoining oceanic region north of about 8°N while a moderate dry anomaly zone exists over the eastern equatorial Indian Ocean. The convection during the active period is intense over most of the Indian subcontinent and over the Arabian Sea and Bay of Bengal. This pattern with opposite sign is seen during the break phase with moderate convection over the equatorial Indian Ocean and strong dry anomalies over India.

By using rainfall index over India (i.e., IMR index) to identify the active and break phases, the composites of OLR anomalies in Fig. 1a seem to have captured the wet and dry zones in appropriate locations. The importance of using the rainfall index is demonstrated by showing OLR composites based on other definitions of active and break phases. One such definition of the active and break periods by Goswami and Ajaya Mohan (2001) is based on 30-60 day band-pass filtered 850 hPa zonal wind at the point (90°E, 15°N). The composites of daily OLR anomalies constructed using their active and break definition (dates provided by B. N. Goswami

and R. S. Ajaya Mohan, private communication) for 1978-1997 are shown in Fig. 1b. During the active phase, most of India is dry and convection is confined to the head of Bay of Bengal, near the location where the active/break index is defined. The positive anomalies over the Indian Ocean cover a much larger region including part of the Arabian Sea. The pattern is reversed with anomalies of opposite sign in the break composite (Fig. 1b).

Another definition of active and break phases is based on the values of 850 hPa zonal wind and OLR in the region (65°E–95°E, 10°N–20°N) and 850 hPa meridional wind at (45°E, 0) (Webster et al. 1998). The composites of OLR anomalies constructed for 1980-1993 (using dates from Table 7 of Webster et al. 1998) show a strong convection zone confined to the region (65°E–100°E, 5°N–20°N) during the active period (Fig. 1c). The region north of 20°N over India has almost no convection. The positive anomalies over the Indian Ocean are very weak and lie to the south of the equator. The pattern is reversed with opposite sign anomalies during in the break composite (Fig. 1c). The three sets of composites in Fig. 1 show that the locations of wet and dry zones depend on the location used in the definition of active and break phases.

b. Evolution of OLR anomalies during active and break phases

The previous discussion points to the importance of defining the active and break phases in terms of rainfall over India. The evolution of convection over the Indian Ocean corresponding to the active and break life cycles of rainfall over India has not been shown in previous studies. Such a description will be useful in proper understanding of the establishment of active and break phases over India starting with convection over the Indian Ocean. Lagged composites of daily OLR anomalies constructed with respect to the midpoint (lag 0) of active and break rainfall phases identified in this study for JJAS 1975-2002 are presented in Fig. 2. At lag −12 days, a

convection zone appears in the Indian Ocean with two centers, one near the west coast of India and the other to the south of Bay of Bengal, while the northern Bay of Bengal and a large area of the Indian subcontinent are dry regions (Fig. 2a). During lags −10 to −6 days, the region of convection expands and acquires a northwest-southeast orientation from equator to 25°N with increased strength. While the central peak over the Arabian Sea and the west coast of India expands but remains stationary, the other center has moved from the equatorial Indian Ocean to the east coast of India and Bay of Bengal. At the same time, the dry region over the northern Bay of Bengal has diminished and moved over to the foothills of the Himalayas. The two centers of convection merge and expand in all four directions covering almost the entire Indian subcontinent, the Bay of Bengal and the Arabian Sea from lags −4 to 0. The southern edge of the convection area has moved a few degrees north of the equator during this period. A weak dry zone appears in the equatorial Indian Ocean at lag −4 days and subsequently expands and intensifies. By lag 0, the strong dry anomalies are concentrated in the equatorial region 80°E–100°E. The convection anomalies over India weaken during lag +2 to +4 days and their meridional extent reduces to cover only region near the foothills of the Himalayas. By lag +4 days, the drier anomalies over the Indian Ocean have expanded in the meridional direction.

The lagged composites of OLR anomalies during the break phase show both structure and evolution similar to those during active phase except with opposite sign (Fig. 2b). The evolution of convection anomalies over India during the active and break periods has good correspondence with the lag composites of rainfall anomalies over India shown by Krishnamurthy and Shukla (2005). Some features of Fig. 2 are similar to those shown by Lawrence and Webster (2002). The life cycles of OLR anomalies during active and break phases contain intraseasonal variations of different time ranges. The discussion in the next section will

reveal such oscillations as well as the presence of large-scale modes that persist throughout the monsoon season.

4. MSSA of OLR anomalies

The space-time structure of the intraseasonal variability over the larger monsoon region was determined by applying MSSA to daily OLR anomalies in the region (40°E–160°E, 20°S–35°N) for the period JJAS 1975–2002 with a lag window of 61 days. The analysis has followed exactly the same procedure used with the rainfall data by Krishnamurthy and Shukla (2005) and based on the discussion of Ghil et al. (2002). Each ST-EOF consists of a sequence of 61 lagged maps and the corresponding ST-PC is 62 days long each year. Using the ST-EOF and ST-PC, the space-time RC, denoted by $R(i)$ for eigenmode i, was computed for different eigenmodes. Each RC has exactly the same time-length and sequence as the original time series and represents the corresponding eigenmode in the total anomalies. This splitting of the original time series into components will help in understanding the space-time structure of each eigenmode.

a. Eigenmodes

The first 30 eigenvalues of the spectrum of explained variance from the MSSA of daily OLR anomalies are plotted in Fig. 3a, as percentage fraction of the total variance. The first six eigenmodes explaining about 16.2% of the variance were found to be the most relevant to describe the dominant variability of the OLR anomalies. The consecutive eigenmodes with almost equal eigenvalues that satisfy the criteria to be oscillatory, as specified by Plaut and Vautard (1994), are the pairs (1, 2) and (5, 6). The eigenmodes 3 and 4 are non-oscillatory but are important components of the variability throughout the monsoon season. The power spectra

of the six eigenmodes are plotted in Fig. 3b showing that pairs (1, 2) and (5, 6) have broad spectra centered around 45 and 28 days, respectively. The power spectrum of each mode was computed by applying FFT to the first spatial principal component (S-PC 1) of the mode's RC. Although their spectra and broad and overlap to some extent, the pairs (1, 2) and (5, 6) will be referred to as 45-day and 28-day oscillatory modes, respectively, for convenience. The spectra of eigenmodes 3 and 4 are red, indicating the possibility that the modes are persisting standing patterns. More detailed space-time spectra of these modes will be discussed later.

b. Intraseasonal oscillatory modes

The RC for an oscillation is simply the sum of the RCs of the individual eigenmodes of the pair. Denoting $R(i) + R(j) = R(i, j)$, the RCs of 45-day and 28-day oscillations are $R(1,2)$ and $R(5,6)$, respectively. The daily phase angle θ of the oscillations were computed from the RCs following the method used by Krishnamurthy and Shukla (2005). It must be emphasized that these two oscillations vary in a nonperiodic manner at the time scale indicated by their broad spectra shown in Fig. 3b. It is easy to follow the space-time structure of the oscillatory mode during an average period by constructing composites of $R(1,2)$ and $R(5,6)$ for chosen intervals of the phase of the respective mode. In a cycle of $(0, 2\pi)$, θ is divided into eight intervals in the range $(k-1)\pi/4 \le \theta(t) \le k\pi/4$ with $k = 1, 2, \ldots, 8$. By averaging the RC for all times during the phase k, the phase k composite is obtained for each oscillatory mode.

The composites of $R(1,2)$ for eight phases of a cycle of (1,2) oscillatory mode are shown in Fig. 4. The average period of this cycle is 45 days. The composites of phases 1 to 4 are almost mirror images of those in phases 5 to 8. The composites reveal the development, maturity and demise of active and break phases over India and help in understanding the associated

convective activity over the larger monsoon region. The phase 1 composite shows the appearance of weak convection in the equatorial Indian Ocean while a dry region with strong anomalies stretch over the entire zonal extent of the domain shown in a northwest-southeast orientation to the north of 5°N. This phase with intense dry anomalies over India represents the peak of the break phase of the monsoon. The convection over the Indian Ocean intensifies and expands in all directions during phases 2 and 3 while the dry anomalies over India weaken and shrink in spatial extent covering only parts of northern India and the head of Bay of Bengal. Over the western Pacific, the dry anomalies however remain strong and the weak convection in the northern part has moved west. During the expansion of the convection area over the Indian Ocean in phase 3, a separate peak appears near the west coast of India. In phase 4, convection further intensifies and stretches from 60°E to 160°E in a northwest-southeast direction. This band has peaks on either sides of the Indian peninsula and the southern edge is above the equator to the west of 90°E. While the dry anomalies over the western Pacific have weakened during phase 4, a very weak dry zone appears along the equator to the east of African coast. Phase 5 shows a slight northward shift of the strong convection band that covers most of India. At the same time, the dry anomalies over the equatorial Indian Ocean have become moderate in intensity and cover an expanded region with peak values near 80°E. The dry zone over the western Pacific has weakened and moved north. Phase 5 represents the peak of the active monsoon period over India. From phase 6 to phase 1, the development of the break phase follows the same route as the development of the active phase but with anomalies of opposite sign. The composites of the 45-day oscillatory mode (1,2) clearly bring out the large-scale extent of the convection covering the Indian Ocean and the West Pacific during the active and break phases that could not seen in the total OLR anomalies in Fig. 2.

The composites of $R(5,6)$ for the eight phases of the oscillation (5,6) shown in Fig. 5 also correspond to a cycle of active and break phases. The average period of this cycle is 28 days. However, there are some differences compared to the cycle of $R(1,2)$ shown in Fig. 4 in terms of the intensity and the spatial extents of convection and dry areas. Phase 1 shows a quadrupole structure with $R(5,6)$ anomalies of moderate intensity. Such quadrupole structure was also seen in the analysis of filtered data by Annamalai and Sperber (2005). The convection zone over the Indian Ocean intensifies and expands during phases 2 and 3 while dry anomalies over India diminish and shift northeastward. Most of the western Pacific is covered with dry anomalies by phase 3. During phase 4, convection over the Indian Ocean weakens somewhat and shifts northward covering most of the Indian subcontinent along with the appearance of two peaks on either side of the Indian peninsula. A weak dry anomaly zone appears at the same time in the equatorial Indian Ocean near the African coast. The quadrupole structure is reestablished in phase 5 but with anomalies of opposite sign compared to phase 1. Thus the quadrupole structures of phase 1 and phase 5 correspond to the peak phases of break and active monsoon periods, respectively. The structure and evolution of $R(5,6)$ during phase 6 to phase 1 corresponds to the establishment of the break monsoon phase over India and follows the same path as in the establishment of the active phase but with anomalies of opposite sign. The convection and dry anomalies of $R(5,6)$ over India during the peak active and break phases (Fig.5) are less intense than in the case of the 45-day oscillation with $R(1,2)$ (Fig. 4). The 45-day and the 28-day modes are part of the total OLR anomalies, and their combination, including the possible interaction between them, should account for the active and break life cycles shown in Fig. 2.

The space-time structure of the two oscillatory modes of the OLR anomalies are now shown to be directly related to the actual daily rainfall anomalies over the Indian subcontinent. With the ISLSCP project rainfall data, the phase composites of daily total rainfall anomalies for the eight phases of OLR $R(1,2)$ and $R(5,6)$ oscillatory cycles were constructed, as shown in Fig. 6. The space-time structures of the rainfall composites in Fig. 6a and 6b show excellent agreement with their counterparts of OLR RCs (Fig. 4 and 5) in depicting the active and break cycles. The peaks of the active and break phases, the rain shadow region in southeastern India and the northern movement of the rainfall anomalies are all captured remarkably well. The rainfall anomalies are more intense during 45-day cycle (Fig. 6a) than during the 28-day cycle (Fig. 6b). The rainfall composites in Fig. 6 have very good correspondence to the composites of RCs of daily rainfall anomalies found in the MSSA of 70-year rainfall data in an earlier study by Krishnamurthy and Shukla (2005).

c. Eigenmodes with seasonally persisting signature

The eigenmodes 3 and 4 are non-oscillatory and can be best described by showing the dominant patterns of the daily RCs, $R(3)$ and $R(4)$ respectively. The spatial EOF analysis of the RCs for 1975-2002 shows that EOF 1 of $R(3)$ and $R(4)$ explain about 91% and 90% of their respective variance. The spatial EOF 1 of $R(3)$ and $R(4)$ reveal distinctly different patterns as seen in Fig. 7. The pattern of $R(3)$ covers the entire domain with anomalies of same sign except for a small area in the equatorial West Pacific. This pattern has stronger anomalies to the north of 10°S except for a small region in the northern Bay of Bengal. The EOF of $R(4)$ in Fig. 7 has a dipole pattern in the equatorial Indian Ocean. Also, strong anomalies, with the same sign as those in the western part of the dipole, exist in a zonal stretch covering most of India and the

west Pacific north of 10°N. The dipole structure in OLR data has also been reported by Gadgil et al. (2004). However, the present study has shown that the dipole structure is a distinct eigenmode of the daily variation of the OLR. The daily variation of these patterns was studied by examining the corresponding PC 1 for the entire period. Each PC 1 varies without any oscillatory behavior, often with the same sign, throughout most of the JJAS season. However, during any particular year, the PC of $R(3)$ may or may not persist with the same sign as that of $R(4)$ through the season. The relative role of the two modes becomes important in determining the seasonal mean. This point will be discussed later with examples during certain years.

To distinguish the character of the oscillatory modes $R(1,2)$ and $R(5,6)$ and the non-oscillatory modes $R(3)$ and $R(4)$ with respect to the monsoon rainfall over India, the daily and seasonal composites were examined. Such an analysis will also indicate whether or not the oscillatory modes possess any seasonal signature. The active and break phase composites of daily values of the RCs were constructed for JJAS 1975-2002 using the earlier identification of active and break days based on the IMR index. The (active − break) difference composites of the RCs thus constructed are plotted in Fig. 8a. The (active − break) composites of daily $R(1,2)$ and $R(5,6)$ are similar to the patterns of these modes during the peak periods (phase 5 − phase 1) of phase composites in Figs. 4 and 5, respectively. The (active − break) composites of daily $R(3)$ and $R(4)$ in Fig. 8a are similar to the dominant EOF patterns of $R(3)$ and $R(4)$ in Fig. 7. The magnitudes of $R(1,2)$ and $R(5,6)$ are about four times bigger than those of $R(3)$ and $R(4)$, indicating the relative roles of the modes in the daily variability.

To study the seasonal mean features of the modes, JJAS seasonal means of the RCs were computed for each year. The composites of the seasonal mean RCs for strong and weak monsoon years were constructed. The strong (weak) monsoon year was selected by using the

criterion that the JJAS seasonal IMR index was greater (less) than one positive (negative) standard deviation of IMR. The (strong − weak) difference composites of the seasonal mean RCs are shown in Fig. 8b. The seasonal composites of $R(1,2)$ and $R(5,6)$ in Fig. 8b show no resemblance to their respective daily composites in Fig. 8a, suggesting the absence of seasonal signature in these modes. The seasonal composites of $R(3)$ and $R(4)$ (Fig. 8b), however, have close spatial resemblance to their daily composites (Fig. 8a), strongly suggesting the presence of persisting signature throughout the monsoon season. The seasonal composites of $R(3)$ and $R(4)$ have much higher magnitude than those of $R(1,2)$ and $R(5,6)$ (note the differences in the scales shown in Fig. 8). The relative contributions of these different components in determining the seasonal mean monsoon will be discussed later.

d. Propagation characteristics

Although several studies indicate northward and eastward propagation of convection from the Indian Ocean to the Indian subcontinent, as described in the introduction, there are differences in the characterization and the association between the northward and eastward propagation. In addition, studies also reported weak westward and independent northward propagation. The discussion of the space-time evolution of OLR anomalies (Fig. 2) and the phase composites of the 45-day and 28-day oscillations (Figs. 4 and 5) showed that in-situ expansion and contraction of the convection and dry regions in both zonal and meridional directions was the most prominent feature. Movements in northward and eastward directions were noted with $R(1,2)$ and $R(5,6)$ along with westward movement with $R(5,6)$. The propagation characteristics of the eigenmodes are further investigated by examining the wavenumber-

frequency spectra and Hovmoller diagrams of the RCs. For proper interpretation, the results of these analyses must be considered along with the phase composites given in Figs. 4 and 5.

The wavenumber-frequency spectra were calculated for RCs averaged over (40°E–160°E) to obtain the features of north-south propagation in the domain (20°S–35°N). The east-west propagation features in the domain (40°E–160°E) are obtained from the spectra of RCs averaged over (20°S–35°N). The spectra are plotted in Fig. 9 where wavenumber 1 corresponds to the zonal or meridional extent of the region considered. The broad spectra of $R(1,2)$ in Figs. 9a and 9b show that the (1,2) mode is associated with northward and eastward movement with a period centered at 45 days. The spectra of $R(5,6)$ in Figs. 9c and 9d indicate northward movement as well as predominantly westward movement with a period centered at 28 days. The spectra of $R(3)$ and $R(4)$ in Figs. 9e–9h show that they correspond to standing patterns without oscillatory behavior.

The variations in propagation features can be better seen in the Hovmoller diagrams of the RCs. To show the average behavior for the entire 1975-2002 period, the phase of the oscillatory modes in a cycle is used as the time coordinate. The longitude-phase cross-sections of $R(1,2)$ and $R(5,6)$ averaged over the latitudinal belts (5°S–10°N) and (10°N–25°N) are plotted in Fig. 10. These diagrams show the propagation for an average cycle moving forward in time from phase $-\pi$ to $+\pi$. The (1,2) mode exhibits eastward propagation over the Indian Ocean and the West Pacific in the (5°S–10°N) belt whereas there are standing patterns separated at 100°E in the (10°N–25°N) belt. The (5,6) mode has a standing pattern to the west of 100°E and eastward movement to the east of 100°E in (5°S–10°N). In the (10°N–25°N) belt, there is a suggestion of weak eastward movement to the west of 100°E and westward propagation in the western Pacific for the (5,6) mode. In order to show that these same features in real time, the corresponding

longitude-time cross-sections for JJAS 1987 are plotted in Fig. 11. The propagation features of Fig. 10 are also clearly seen in Fig. 11 along with the period of each mode.

The northward or southward movement of the 45-day and 28-day oscillatory modes are examined from the phase-latitude cross-sections of $R(1,2)$ and $R(5,6)$ averaged over (60°E–100°E) and (100°E–160°E) in Fig. 10. In the (60°E–100°E) belt that contains the Indian Ocean and the Indian subcontinent, both the oscillatory modes have southward movement to the south of the equator and northward movement to the north of the equator. In the western Pacific belt of (100°E–160°E), these modes show northward propagation from 10°S to 25°N. The same propagation characteristics are also revealed in the time-latitude cross-sections for JJAS 1987 shown in Fig. 11. Although these diagrams may indicate clear propagation in certain directions, a complete picture involves considerable in-situ expansion or contraction.

e. Seasonal mean monsoon

The relative contribution of the oscillatory and the non-oscillatory modes in determining the seasonal mean monsoon over India is now discussed. For this purpose, the RCs are averaged over the land points in India exactly like the IMR index. The daily variations of these all-India averaged RCs of the modes are examined in detail for two particular years, as shown in Fig. 12 for the weak monsoon year 1987 and strong monsoon year 1988. Throughout the JJAS season, $R(1,2)$ and $R(5,6)$ fluctuate approximately near zero with the time scale of about 45 and 28 days, respectively. While the number of cycles of fluctuations is the same for the two years for each mode, the amplitudes are bigger during the weak year than those during the strong year. It is important to note that these fluctuations are not periodic and do not vary in a sinusoidal manner about zero. Therefore, the seasonal mean does not add up to zero. The more interesting

behavior is seen in $R(3)$ which has strong positive (negative) values throughout JJAS of 1987 (1988), clearly showing season-long persistent signature consistent with the seasonal mean character of the monsoon rainfall for the year. Somewhat similar behavior is also seen in $R(4)$ which has strong positive anomalies throughout 1987 but is close to zero without fluctuations during 1988.

The spatial structures of the JJAS seasonal means of the RCs for 1987 and 1988 are presented in Fig. 13. The magnitudes of $R(1,2)$ and $R(5,6)$ are about three times smaller than those of $R(3)$ and $R(4)$. The difference between the two years is reflected in a consistent manner for $R(1,2)$ and $R(3)$. However, R(5,6) has higher than normal convection over India during 1988 but is not consistent with the weak year 1987. This situation is opposite for R(4) which shows a dry monsoon over India in 1987 and also weak dry anomalies during 1988. The seasonal mean monsoon may therefore depend on the relative strengths of these components.

In order to get a quantitative understanding of the relative strengths of the different modes, the interannual variability for 1975-2002 was examined. The time series of all-India averages (like IMR index) of JJAS seasonal mean of RCs and total OLR anomalies are plotted in Fig. 14. These time series are also compared with the JJAS seasonal means of IMR index and NINO3.4 index (SST anomaly averaged over 170°W–120°W, 5°S–5°N). The time series of all the OLR anomalies and the NINO3.4 index are plotted with negative sign for easy comparison with the IMR index. In Fig. 14a, it can be seen that the seasonal mean total OLR anomaly is in good correspondence with the IMR index except during 1975-77 and 1997-2000. However, NINO3.4 shows even better correspondence with the total OLR anomaly (Fig. 14b). The oscillatory modes $R(1,2)$ and $R(5,6)$ in Fig. 14c show that the seasonal means are quite small for the entire period and that the interannual variability has no correspondence with other time series

in Figs. 14a and 14b. In fact, their correlations with the time series in Figs. 14a and 14b are insignificant. The seasonal means of the persistent components $R(3)$ and $R(4)$ (Fig. 14c and 14d) have magnitudes comparable to that of the total OLR anomaly (Fig. 14a). $R(3)$ has a correlation of 0.7 with the total OLR anomaly, a correlation of −0.45 with the IMR index and a correlation of 0.91 with NINO3.4 for 1979-2002. The difference in the correlation between OLR and that with IMR comes mainly from the disagreement between the rainfall index and OLR index during 1998-2001 (Fig. 14a), the same period during which the OLR anomaly has better correspondence with the NINO3.4 index (Fig. 14b). The correlation between $R(4)$ and the total OLR anomaly is quite low (0.23) while $R(3)+R(4)$ increases the correlation to 0.75.

Although the interannual variability of $R(4)$ is not well correlated with the Indian monsoon, it plays a significant role during certain years (e.g., 1994). The relative values of the all-India averages of daily $R(3)$ and $R(4)$ throughout the JJAS season for all years were examined. The daily all-India averages of $R(3)$ and $R(4)$ are plotted in Fig. 15 for three each of weak, strong and normal monsoon years. $R(3)$ has seasonally persistent variation consistent with all the weak years (Fig. 15a) and for most of the strong years except 1994 (Fig. 15c). For normal years, $R(3)$ is persistent with strong anomalies of same sign throughout the season and reflects the variation of NINO3.4 (Fig. 15e). The variation of $R(4)$ during weak and strong years (Figs. 15b and 15d) is not consistent with the variations of the total OLR anomaly except for 1987 (weak) and 1994 (strong). During normal years, $R(4)$ varies as $R(3)$ during 1999 but with opposite anomalies during other years (Fig. 15f). During the severe drought year of 2002, the persistent drought condition is reflected by $R(3)$ (Fig. 15a) but not by $R(4)$ (Fig. 15b).

5. Summary and conclusions

The main results of this study show that there are two dominant intraseasonal oscillatory modes and two seasonally persisting large-scale standing patterns over the larger Indian monsoon region. Daily observed OLR data were analyzed to understand the intraseasonal space-time structure of convection over the monsoon region that includes the Indian subcontinent and the Indian Ocean. The intraseasonal oscillatory patterns were shown to extend into the West Pacific. A direct relation between convection variability over the larger monsoon region and the rainfall over India was also established. The seasonal mean monsoon was shown to be determined mainly by the two persisting standing patterns, one with the ENSO signature and the other with a dipole pattern over the Indian Ocean.

The two oscillatory modes that emerged from the MSSA of daily OLR anomalies have broad spectral peaks centered at 45 and 28 days. During a cycle of these nonlinear oscillations, both modes reveal the development, maturity and demise of active and break monsoon phases. These OLR oscillatory modes showed excellent correspondence with the rainfall patterns over India in depicting the active and break phases. The 45-day OLR mode is more intense than the 28-day mode. In both the modes, when there is convection over the Indian subcontinent, the equatorial Indian Ocean is dry, and vice versa. The spatial scale of the oscillatory modes extends to the western Pacific with some differences between the two modes. During the peak of the active (break) monsoon period over India, the convection (dry) anomalies of the 45-day mode have a zonal extent ranging 60°E–160°E while the 28-day mode exhibits a quadrupole structure with convection (dry) anomalies over India. The two oscillatory modes with different time scales combine together, perhaps in a nonlinear manner, to determine the space-time evolution of the intraseasonal variability over the larger monsoon region.

For both the oscillatory modes, after a weak convection or dry anomaly zone appears in the equatorial Indian Ocean, it intensifies and expands in both zonal and meridional directions covering a large part of the Indian subcontinent also. Later this convection or dry zone contracts over India with the southern edge moving north. The 45-day mode shows both eastward and northward movement in (0-10°N) and only northward movement north of 10°N when cross-sections are examined. Similar examination showed that 28-day mode has only northward movement over the Indian Ocean and the Indian subcontinent, whereas over the West Pacific, the northward movement is also associated with westward propagation. The propagation characteristics of the oscillatory modes must be interpreted carefully after taking into consideration the predominant in-situ expansion and contraction of convection or dry anomalies.

The oscillatory modes fluctuate about the two standing modes that persist with the same pattern throughout the monsoon season. One of these modes (mode 3) covers the entire region with anomalies of same sign except for a small region in the western Pacific. The spatial structure of mode 3 is related to ENSO and the correlation with NINO3.4 index was shown to be extremely high. The other seasonally persisting standing pattern (mode 4) has a dipole pattern over the Indian Ocean along with anomalies over the entire zonal extent north of 10°N with the same sign as those over the western part of the dipole. The strength of the JJAS seasonal mean OLR anomalies is mainly determined by the two persisting standing patterns (modes 3 and 4) and the contribution from the oscillatory modes is small. The interannual variability of the seasonal mean of total OLR anomaly is best correlated with the ENSO-related mode.

Over the Indian subcontinent, while the 45-day and 28-day oscillatory modes determine the variability of the active and break phases of monsoon, the persisting ENSO-related mode and the dipole mode vary mostly with the same sign throughout the monsoon season. The seasonal

mean monsoon rainfall over India is strongly related to the ENSO-related mode most of the years. Although the interannual variability of the dipole mode is not well correlated with the seasonal mean rainfall over India, it plays a crucial role during certain years, such as 1994 and 1997. Although 1997 was a very strong El Niño year, the Indian rainfall was normal. This observation was generally interpreted as a breakdown of ENSO-monsoon relation. However, this study has shown that the ENSO-related convection mode was still stronger with positive anomalies throughout 1997 but was offset by the dipole mode which persisted with negative anomalies. The most notable result of the MSSA is to distinguish these different modes and point to a possible connection to the oceanic variability.

The results of this study further confirm the hypothesis by Charney and Shukla (1981) that there is potential long-term predictability of monsoon because of the response due to slowly varying boundary forcings. The role of the intraseasonal oscillatory modes cannot be ignored. During the years when the combined effect of seasonally persisting components is relatively weak, the role of oscillatory modes may become important in determining the seasonal mean monsoon. While the indication of the relation between the persisting standing patterns and the oceanic variability is strong, the influence of ocean on the intraseasonal modes also needs investigation. Since the atmospheric dipole mode that emerged in this study is strong during JJAS, it remains to be seen if it is related to the development of the SST dipole in the Indian Ocean that is prominent during the subsequent season. A thorough analysis of the relation between the SST and the OLR modes will be presented in another paper.

Acknowledgments

This research was supported by grants from the National Science Foundation (0334910), the National Oceanic and Atmospheric Administration (NA040AR4310034), and the National Aeronautics and Space Administration (NNG04GG46G). The authors thank B. N. Goswami and R. S. Ajaya Mohan for providing the active and break dates from their work.

References

Annamalai, H., and J. M. Slingo, 2001: Active/break cycles: diagnosis of the intraseasonal variability of the Asian summer monsoon. *Climate Dyn.*, **18,** 85–102.

Annamalai, H., and K. R. Sperber, 2005: Regional heat sources and the active and break phases of boreal summer intraseasonal (30-50 day) variability. *J. Climate.*, **62,** 2726–2748.

Charney, J. G., and J. Shukla, 1981: Predictability of monsoons. *Monsoon Dynamics*, J. Lighthill and R. P. Pearce, Eds., Cambridge University Press, 99–109.

Fu, X., and B. Wang, 2004: Differences of boreal summer intraseasonal oscillations simulated in an atmosphere-ocean coupled model and an atmosphere-only model. *J. Climate*, **17,** 1263–1271.

Fu, X., B. Wang, T. Li, J. P. McCreary, 2003: Coupling between northward-propagating, intraseasonal oscillations and sea surface temperature in the Indian Ocean. *J. Atmos. Sci.*, **60,** 1733–1753.

Gadgil, S., P. N. Vinayachandran, P. A. Francis, and S. Gadgil, 2004: Extremes of the Indian summer monsoon rainfall, ENSO and equatorial Indian Ocean oscillation. *Geophys. Res. Lett.*, **31,** L12213, doi:10.1029/2004GL019733.

Ghil, M., M. R. Allen, M. D. Dettinger, K. Ide, D. Kondrashov, M. E. Mann, A. W. Robertson, A. Saunders, Y. Tian, F. Varadi, and P. Yiou, 2002: *Rev. Geophys.*, **40(1),** 1003, doi:10.1029/2000RG000092.

Goswami, B. N., and R. S. Ajaya Mohan, 2001: Intraseasonal oscillations and interannual variability of the Indian summer monsoon. *J. Climate*, **14,** 1180-1198.

Hartmann, D. L., and M. L. Michelsen, 1989: Intraseasonal periodicities in Indian rainfall. *J. Atmos. Sci.*, **46,** 2838-2862.

Jiang, X., T. Li, and B. Wang, 2004: Structures and mechanisms of the northward propagating boreal summer intraseasonal oscillation. *J. Climate*, **17,** 1022–1039.

Kemball-Cook, S., and B. Wang, 2001: Equatorial waves and air-sea interaction in the boreal summer intraseasonal oscillation. *J. Climate*, **14,** 2923–2942.

Krishnamurthy, V., and J. L. Kinter III, 2003: The Indian monsoon and its relation to global climate variability. *Global Climate*, X. Rodó and F. A. Comín, Eds., Springer-Verlag, Berlin, 186–236.

Krishnamurthy, V., and J. Shukla, 2000: Intraseasonal and interannual variability of rainfall over India. *J. Climate*, **13,** 4366–4377.

Krishnamurthy, V., and J. Shukla, 2005: Intraseasonal and seasonally persisting patterns of Indian monsoon rainfall. *J. Climate* (submitted).

Krishnamurti, T. N., and H. N. Bhalme, 1976: Oscillations of a monsoon system. Part I. Observational aspects. *J. Atmos. Sci.*, **33,** 1937–1954.

Krishnamurti, T. N., and P. Ardanuy, 1980: The 10 to 20-day westward propagating mode and "Breaks in the monsoons". *Tellus*, **32,** 15–26.

Krishnan, R., C. Zhang, and M. Sugi, 2000: Dynamics of breaks in the Indian summer monsoon. *J. Atmos. Sci.*, **57,** 1354–1372.

Lau, K.-M., and P. H. Chan, 1986: Aspects of the 40–50 day oscillation during the northern summer as inferred from outgoing longwave radiation. *Mon. Wea. Rev.*, **114,** 1354–1367.

Lawrence, D. M., and P. J. Webster, 2002: The boreal summer intraseasonal oscillation: Relationship between northward and eastward movement of convection. *J. Atmos. Sci.*, **59,** 1593–1606.

Plaut, G., and R. Vautard, 1994: Spells of low-frequency oscillations and weather regimes in the Northern Hemisphere. *J. Atmos. Sci.*, **51,** 210–236.

Rajeevan, M., 2001: Prediction of Indian summer monsoon: Status, problems and prospects. *Curr. Sci.*, **81,** 1451-1457.

Ramamurthy, K., 1969: Some aspects of the break in the Indian southwest monsoon during July and August. Forecasting Manual, India Meteorological Department, Part IV-18.3.

Thapliyal, V., 1990: Long range prediction of summer monsoon rainfall over India: Evolution and development of new models. *Mausam*, **41,** 339-346.

Sikka, D. R., and S. Gadgil, 1980: On the maximum cloud zone and the ITCZ over Indian longitudes during the southwest monsoon. *Mon. Wea. Rev.*, **108,** 1840–1853.

Singh, S. V., R. H. Kripalani, and D. R. Sikka, 1992: Interannual variability of the Madden-Julian oscillations in the Indian summer monsoon rainfall. *J. Climate*, **5,** 973-978.

Wang, B., and H. Rui, 1990: Synoptic climatology of transient tropical intraseasonal convection anomalies: 1975-1985. *Meteorol. Atmos. Phys.*, **44,** 43–61.

Webster, P. J., V. O. Magaña, T. N., Palmer, J. Shukla, R. A. Tomas, T. M. Yanai, and T. Yasunari, 1998: Monsoons: Processes, predictability, and the prospects for prediction. *J. Geophys. Res.*, **103**, 14451-14510.

Wheeler, M., and G. N. Kiladis, 1999: Convectively coupled equatorial waves: Analysis of clouds and temperature in the wavenumber-frequency domain. *J. Atmos. Sci.*, **56**, 374–399.

Yasunari, T. (1979): Cloudiness fluctuations associated with the northern hemisphere summer monsoon. *J. Meteor. Soc. Japan*, **57,** 227–242.

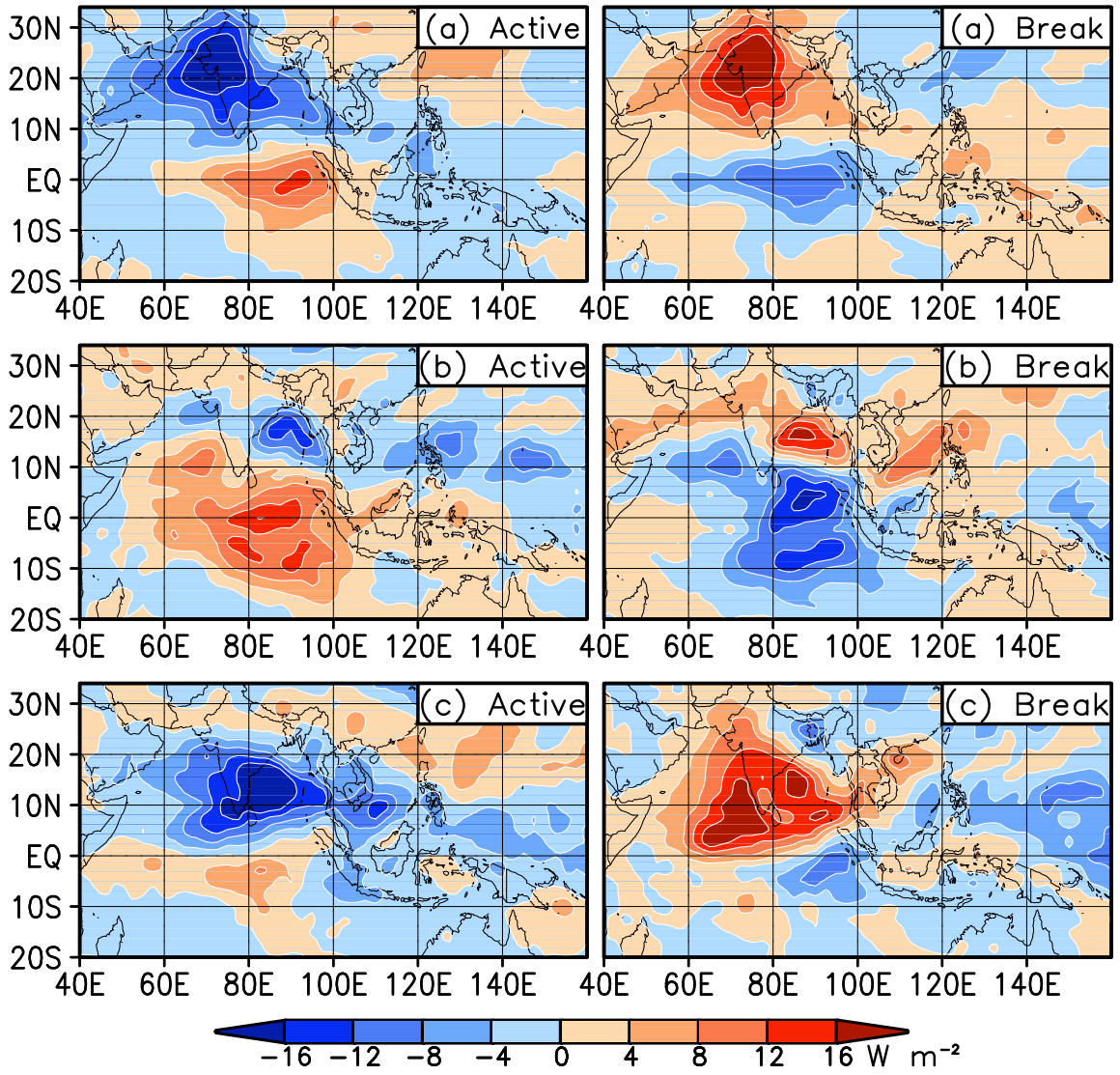

Fig. 1. Active (left panels) and break (right panels) phase composites of OLR (W m^{-2}). The composites in (a) were constructed with the active and break dates, as defined in this study using the IMR index (rainfall anomalies area averaged over India), for JJAS 1975–2002. The composites in (b) and (c) are based on the definition of active and break days by Goswami and Ajaya Mohan (2001) and Webster et al. (1998), respectively.

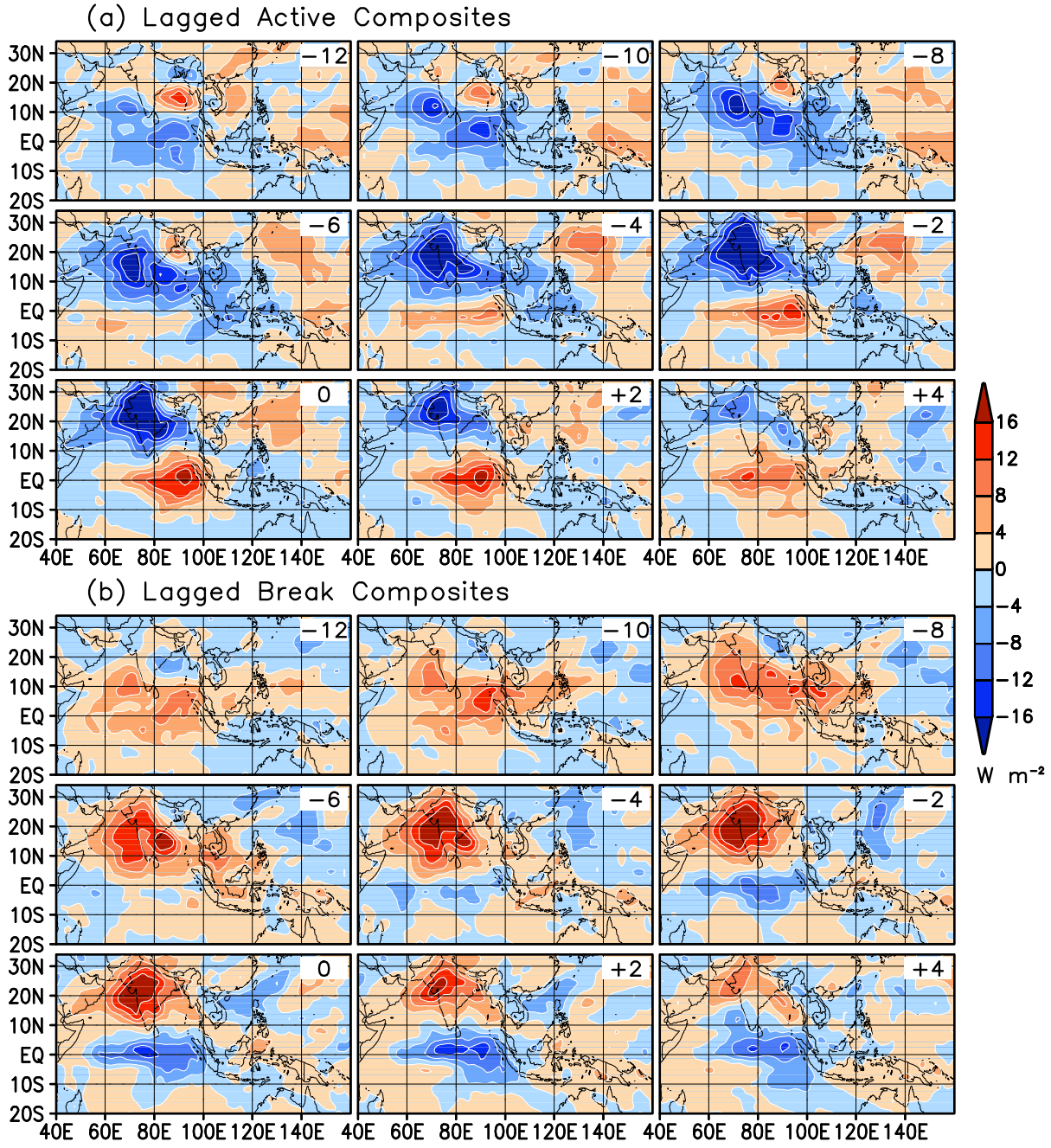

Fig. 2. Lagged active (a) and break (b) phase composites of OLR (W m^{-2}) for JJAS 1975–2002. Lag (–) or lead (+) day is indicated at the top right corner of each panel. Lag 0 corresponds to the midpoint of each active phase.

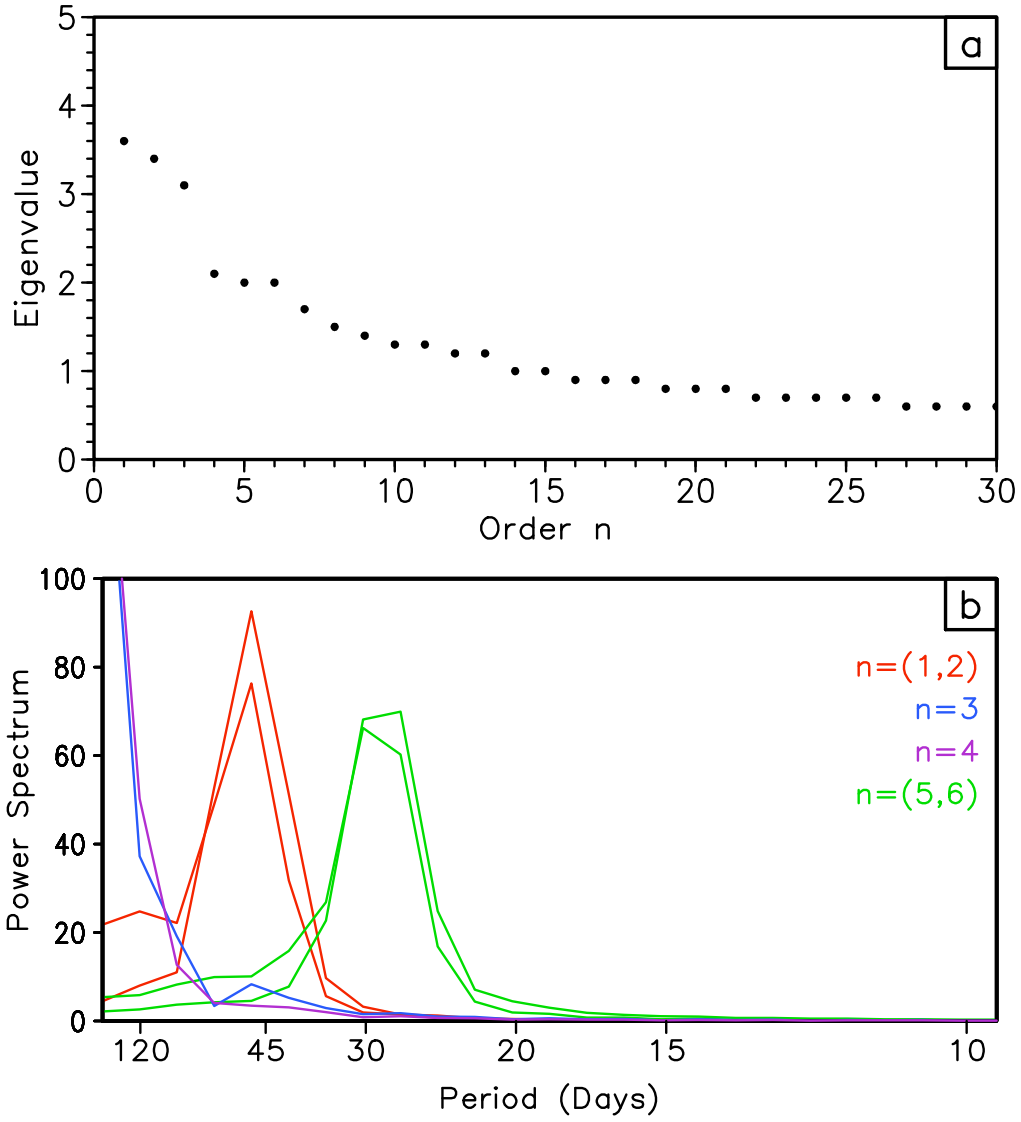

Fig. 3. MSSA of OLR anomaly for JJAS 1975–2002: (a) Eigenvalue spectrum with the first 30 eigenvalues plotted as percentage of the total variance, and (b) power spectra of the S-PC 1 of the first six RCs.

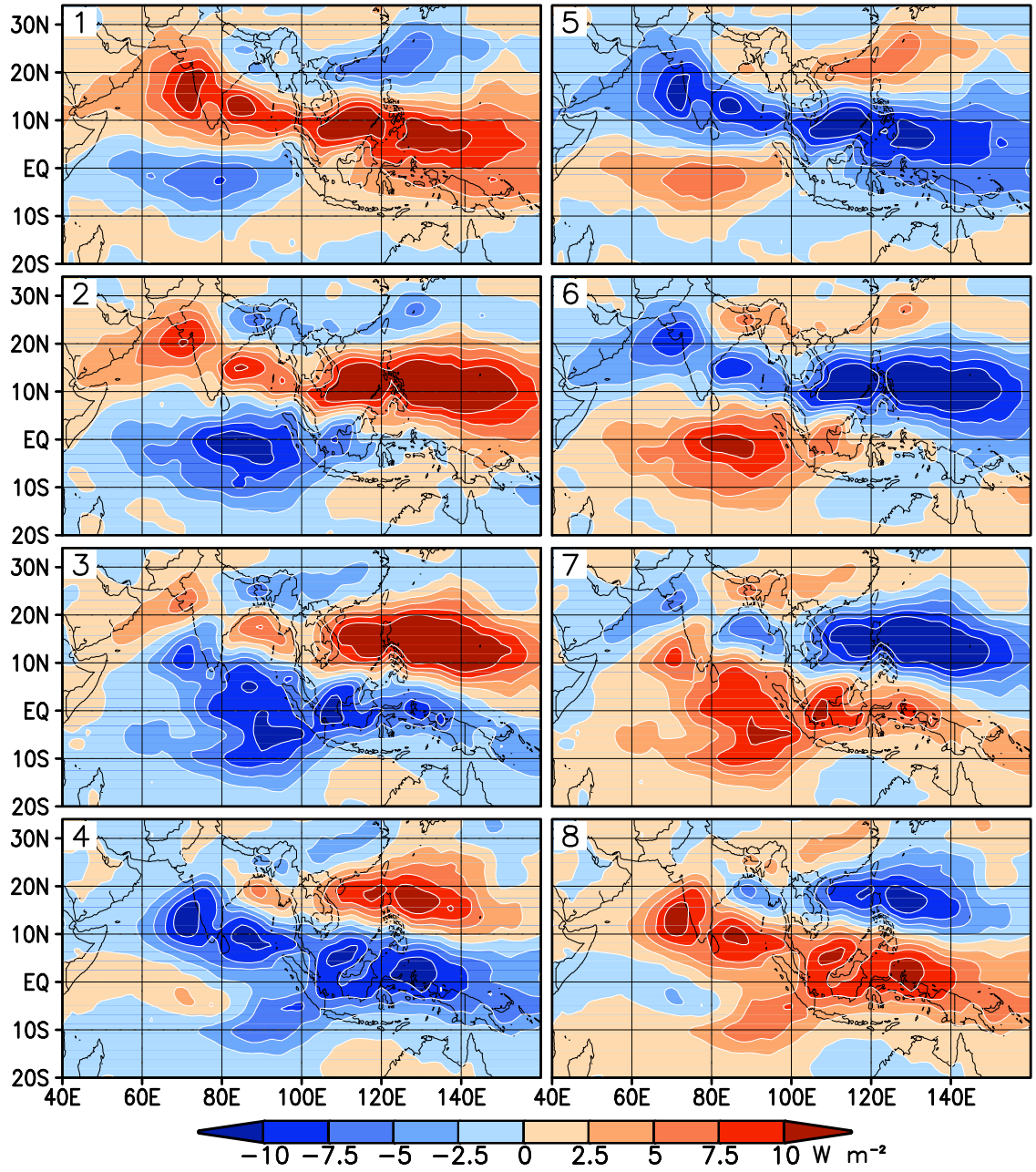

Fig. 4. Phase composites of $R(1,2)$ of the oscillatory mode (1,2) with an average period of about 45 days. Units are in W m^{-2}. The phase number is given at the top left corner of each panel.

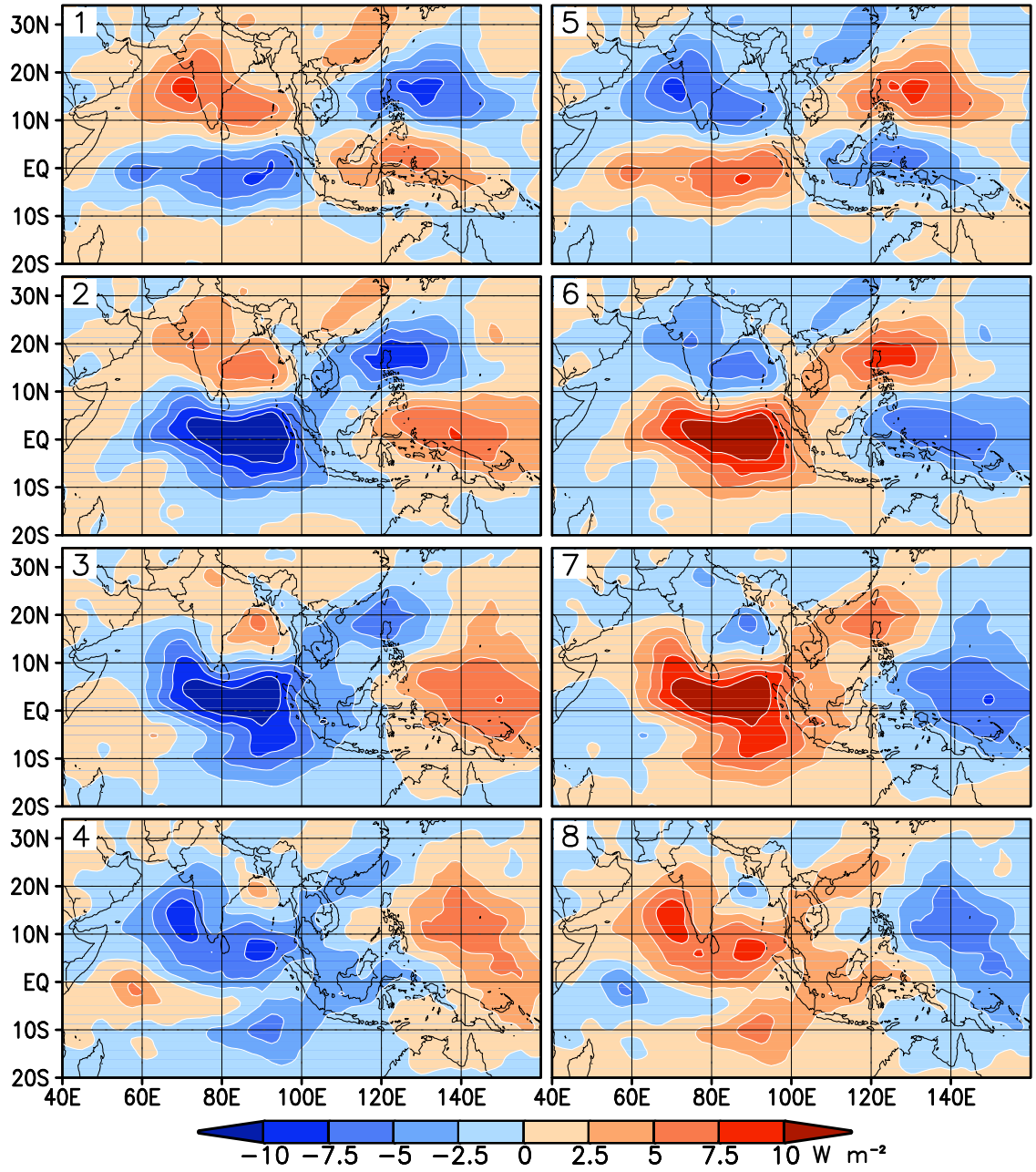

Fig. 5. Phase composites of $R(5,6)$ of the oscillatory mode (5,6) with an average period of about 28 days. Units are in W m^{-2}. The phase number is given at the top left corner of each panel.

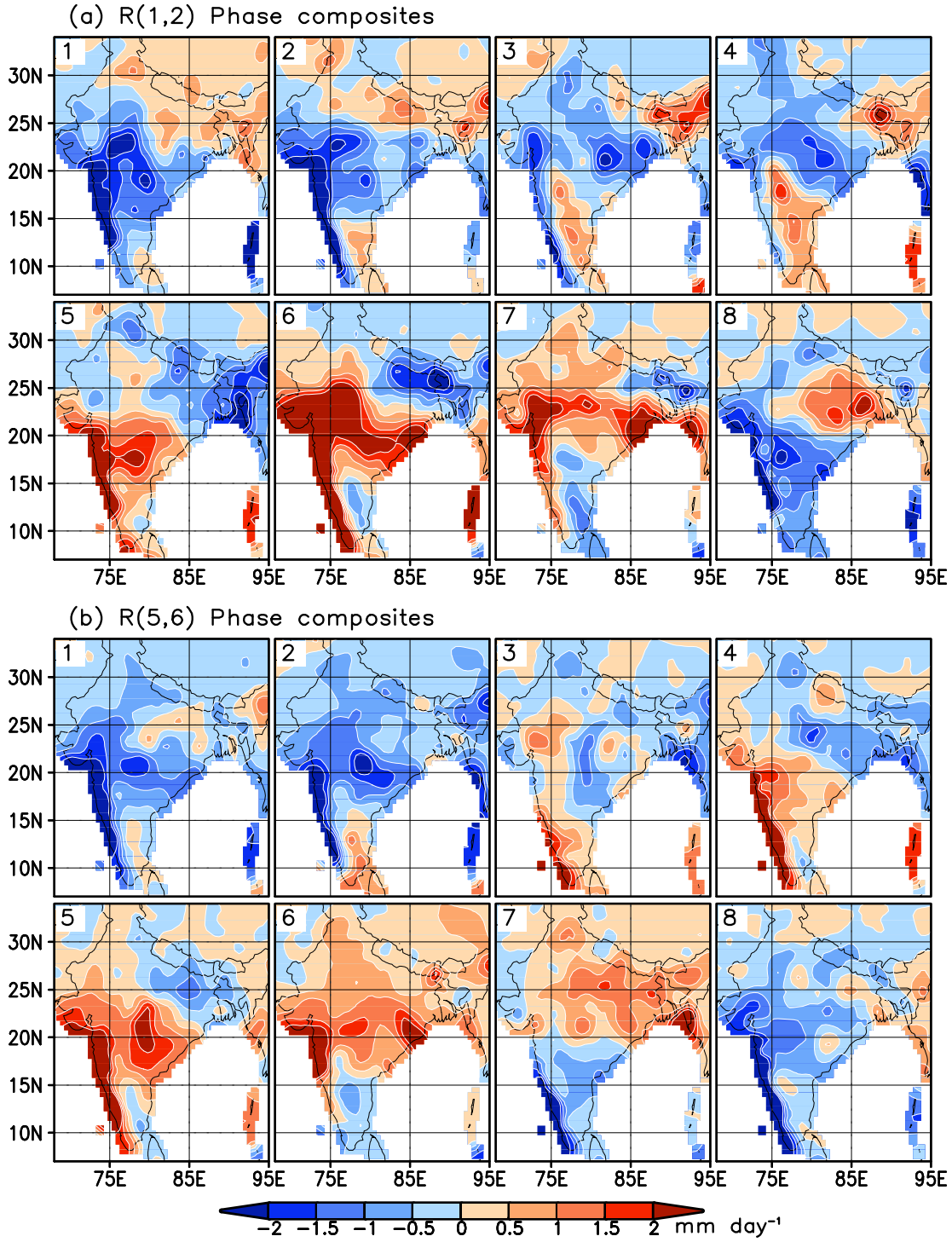

Fig. 6. Composites of rainfall over India for (a) eight phases of the OLR oscillation 1–2 with a period of about 45 days and (b) eight phases of the OLR oscillation 5–6 with a period of about 27 days. Units are in mm d^{-1}. The phase number is given at the top left corner of each panel.

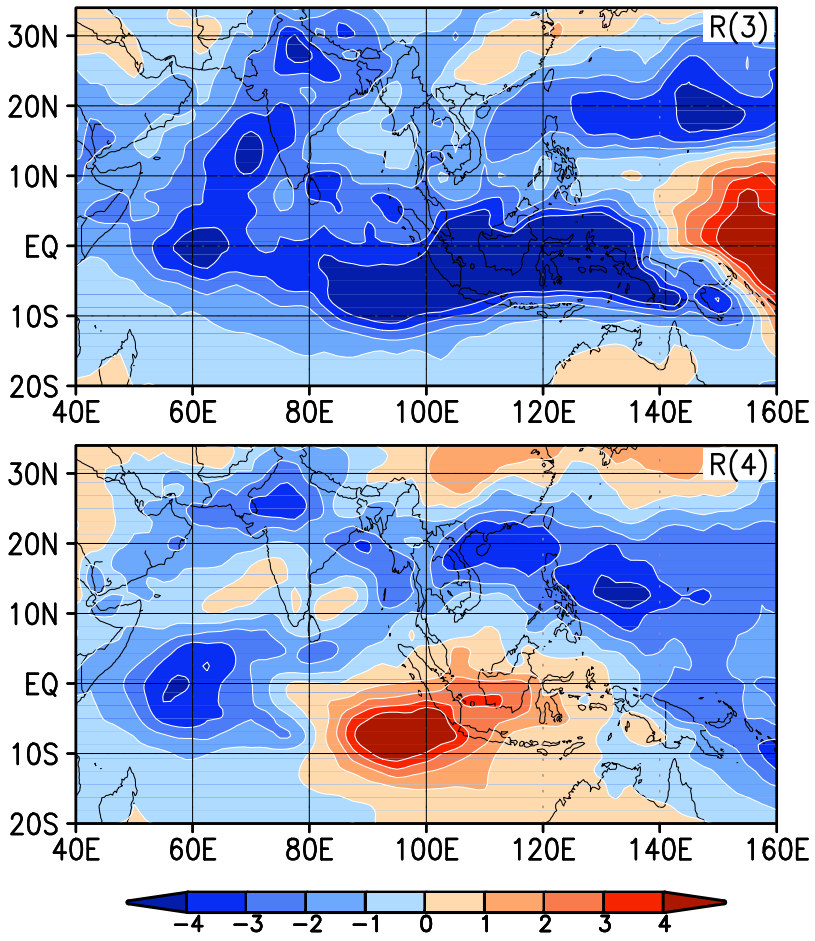

Fig. 7. Spatial EOF 1 of daily $R(3)$ (top) and $R(4)$ (bottom) for JJAS 1975-2002. Units are arbitrary.

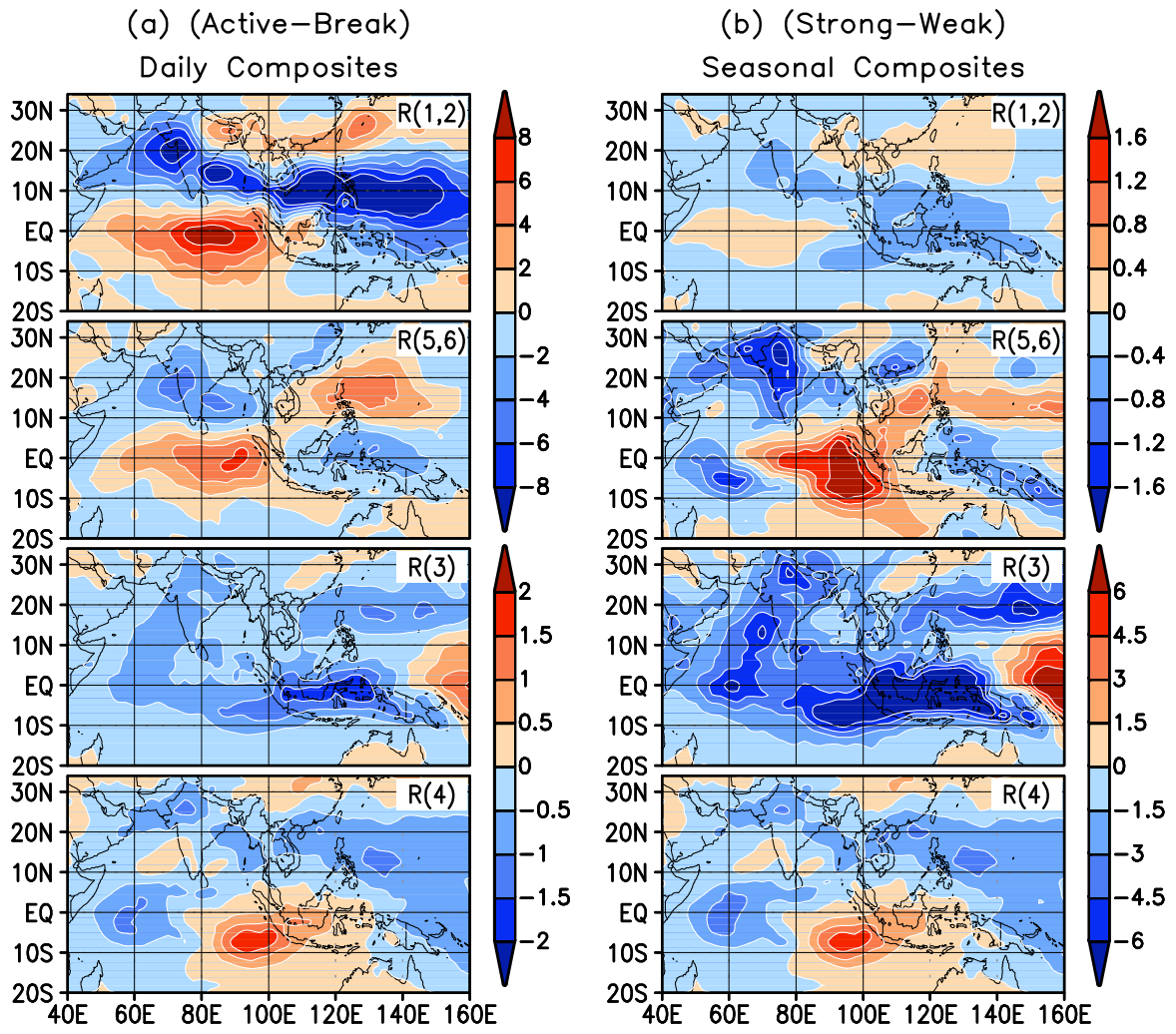

Fig. 8. (a) Difference between active phase composite and break phase composite of daily OLR RCs and (b) difference between strong monsoon year composite and weak monsoon year composite of seasonal mean OLR RCs. The definition of active and break phases are based on the daily rainfall over India and the definition of strong and monsoon are based on the seasonal rainfall over India. The components plotted are identified at the top right corner. Note the difference in scales. The scales for $R(1,2)$ and $R(5,6)$ are given by the top side bars and those for $R(3)$ and $R(4)$ are given by the bottom bars.

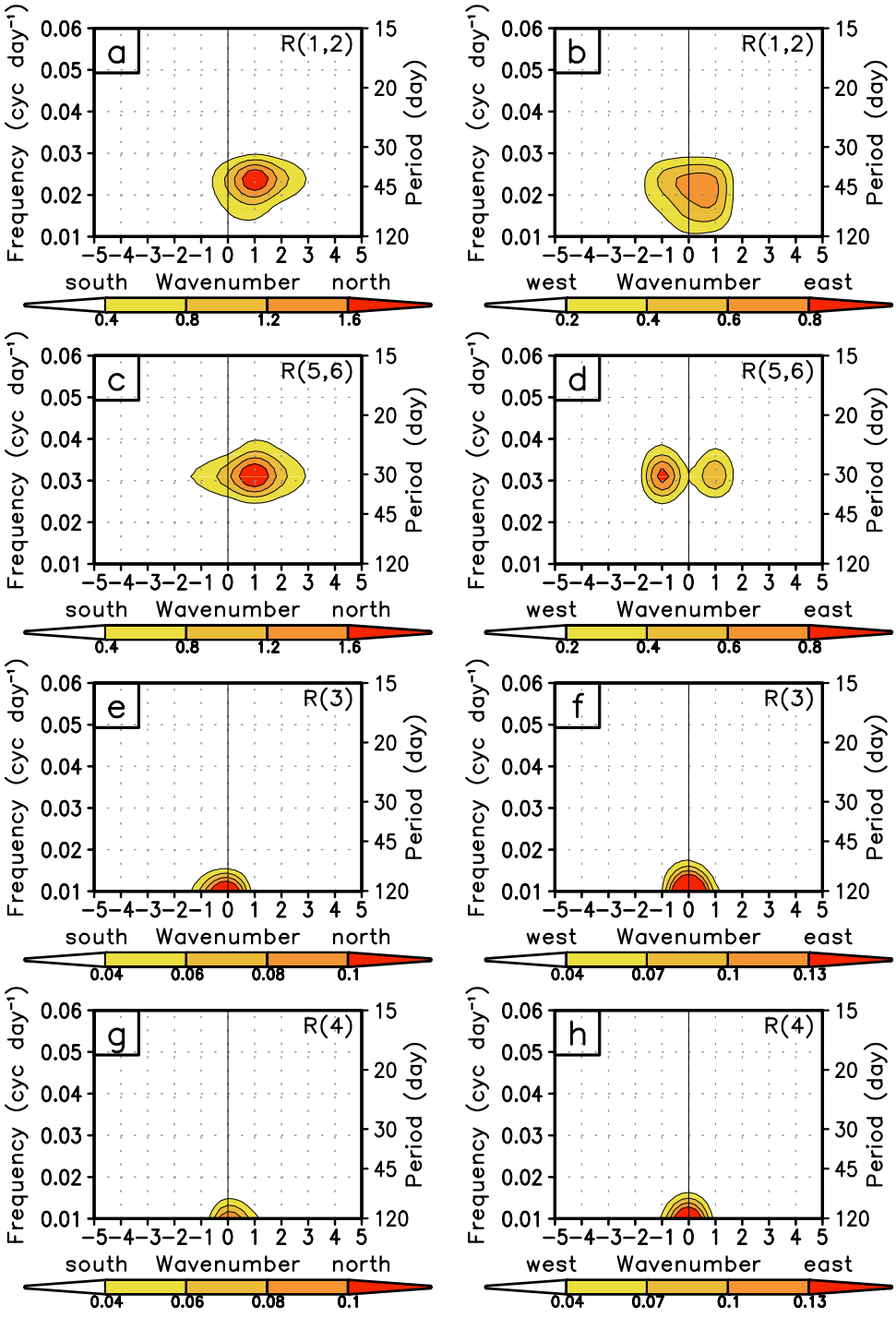

Fig. 9. Wavenumber-frequency spectra from latitude-time domain of (a) $R(1,2)$, (c) $R(5,6)$, (e) $R(3)$ and (g) $R(4)$ and from longitude-time domain of (b) $R(1,2)$, (d) $R(5,6)$, (f) $R(3)$ and (h) $R(4)$ for JJAS 1975–2002. The frequency scale is at left and the period scale at right. See text for the domains for which the spectra are computed.

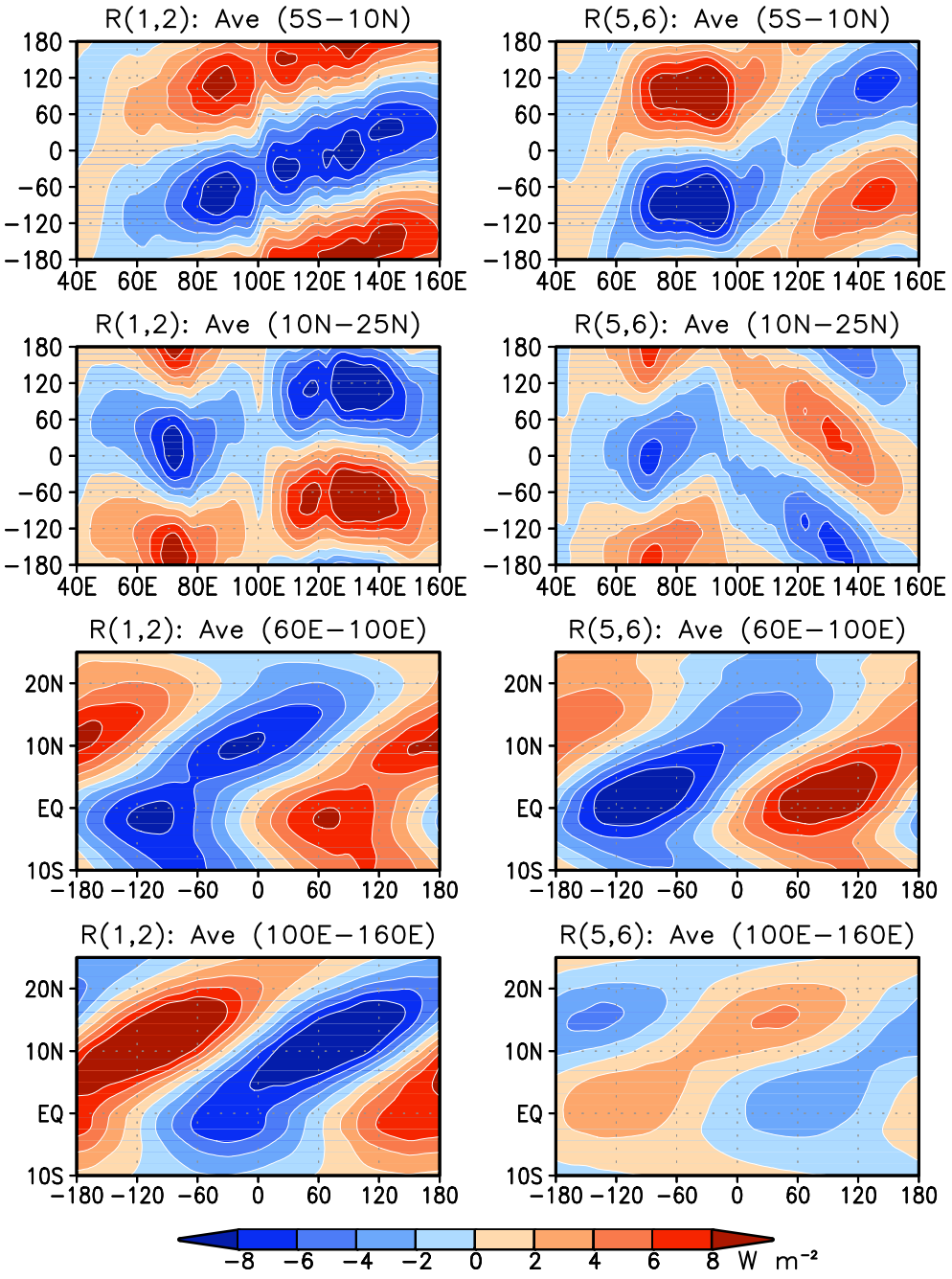

Fig. 10. Cross-sections of phase composites of $R(1,2)$ for a complete cycle of the oscillatory mode (1,2) ranging in phase $-\pi$ to $+\pi$ for the period 1975-2002 are shown in left panels. The composites were constructed at intervals of $\pi/12$. Longitude-time cross-sections of the RC shown in top two panels are averages over (5°S–10°N) and (10°N–25°N). Latitude-time cross-sections of the RCs averaged over (60°E–100°E) and (100°E–160°E) are shown in bottom two panels. Similar composites of $R(5,6)$ for a cycle of the oscillatory mode (5,6) are shown in right panels. The domain of average is indicated at the top of each panel. Units are in W m^{-2}.

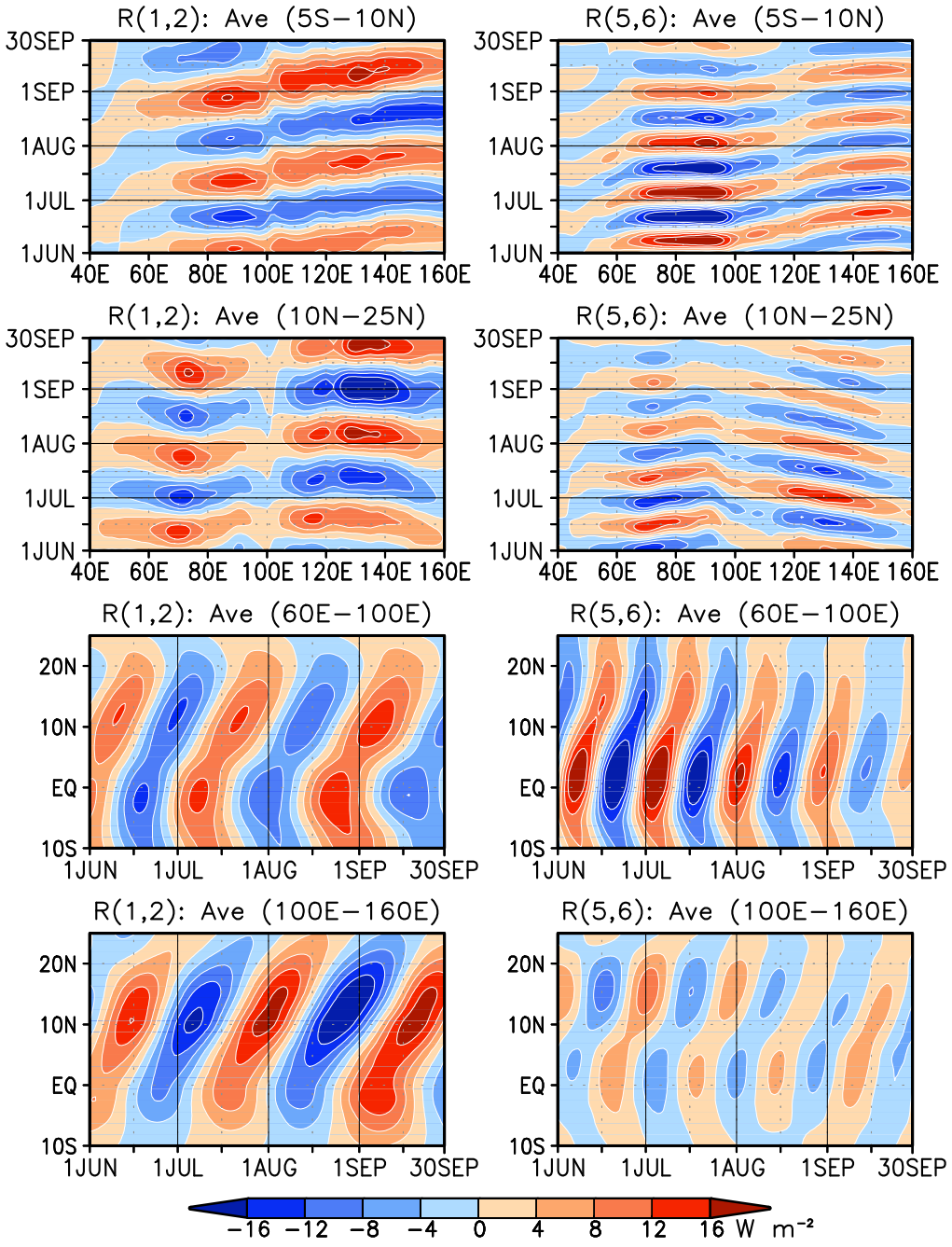

Fig. 11. Cross-sections of daily $R(1,2)$ (left panels) and daily $R(5,6)$ (right panels) for JJAS 1987. Longitude-time cross-sections of the RCs shown in top two panels are averages over (5°S–10°N) and (10°N–25°N). Latitude-time cross-sections of the RCs averaged over (60°E–100°E) and (100°E–160°E) are shown in bottom two panels. The domain of average is indicated at the top of each panel. Units are in W m^{-2}.

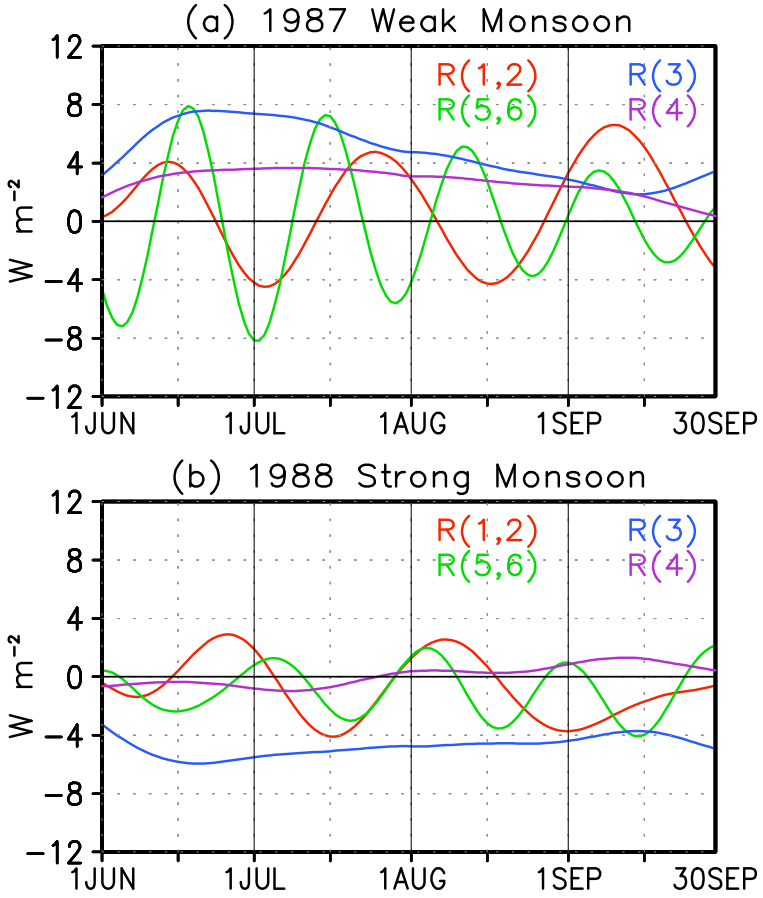

Fig. 12. Time series of daily $R(1,2)$, $R(5,6)$, $R(3)$ and $R(4)$ area averaged over India (as in IMR index). The time series are shown for JJAS of (a) weak monsoon year 1987 (top) and (b) strong monsoon year 1988 (bottom).

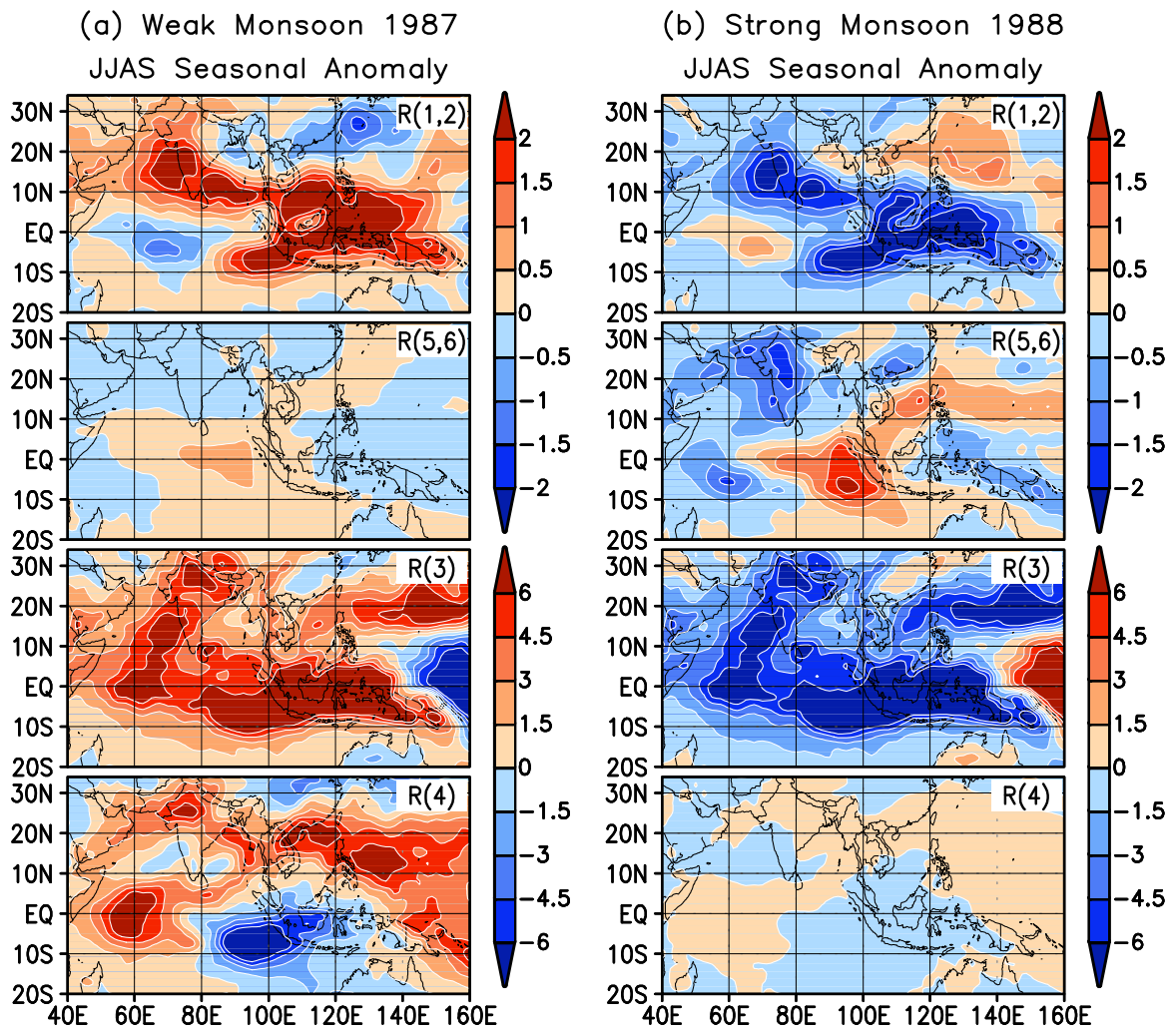

Fig. 13. JJAS seasonal means of OLR RCs for (a) weak monsoon year 1987 (left panels) and (b) strong monsoon year 1988 (right panels). Units are in W m^{-2}. The RC plotted in each panel is identified at the top right corner. Note the difference in scales. The scales for $R(1,2)$ and $R(5,6)$ are given by the top side bars and those for $R(3)$ and $R(4)$ are given by the bottom bars.

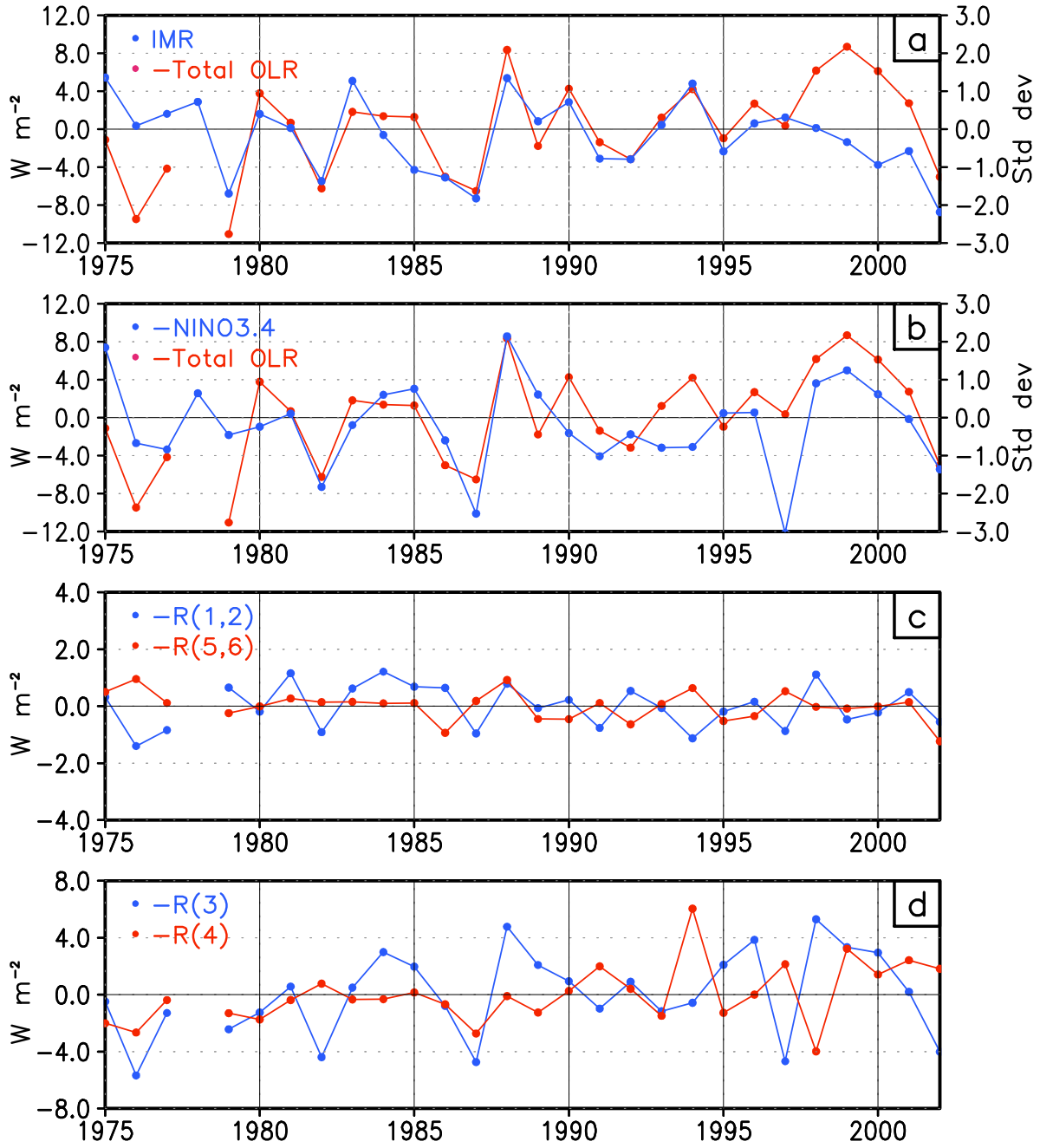

Fig. 14. Time series of JJAS seasonal means of (a, b) total OLR anomaly, (c) *R*(1,2), *R*(5,6), and (d) (*R*(3) and R(4) area averaged over India (IMR region). The time series of JJAS seasonal IMR index (a) and NINO3.4 index (b) are also plotted. The indices and variables plotted are identified in the top left corner in each panel. All the averages except the IMR index are plotted with opposite sign for easy comparison with the rainfall average over India. The scales for the OLR anomalies are given at left. The scales for IMR index and NINO3.4 index are given at right in standard deviation units.

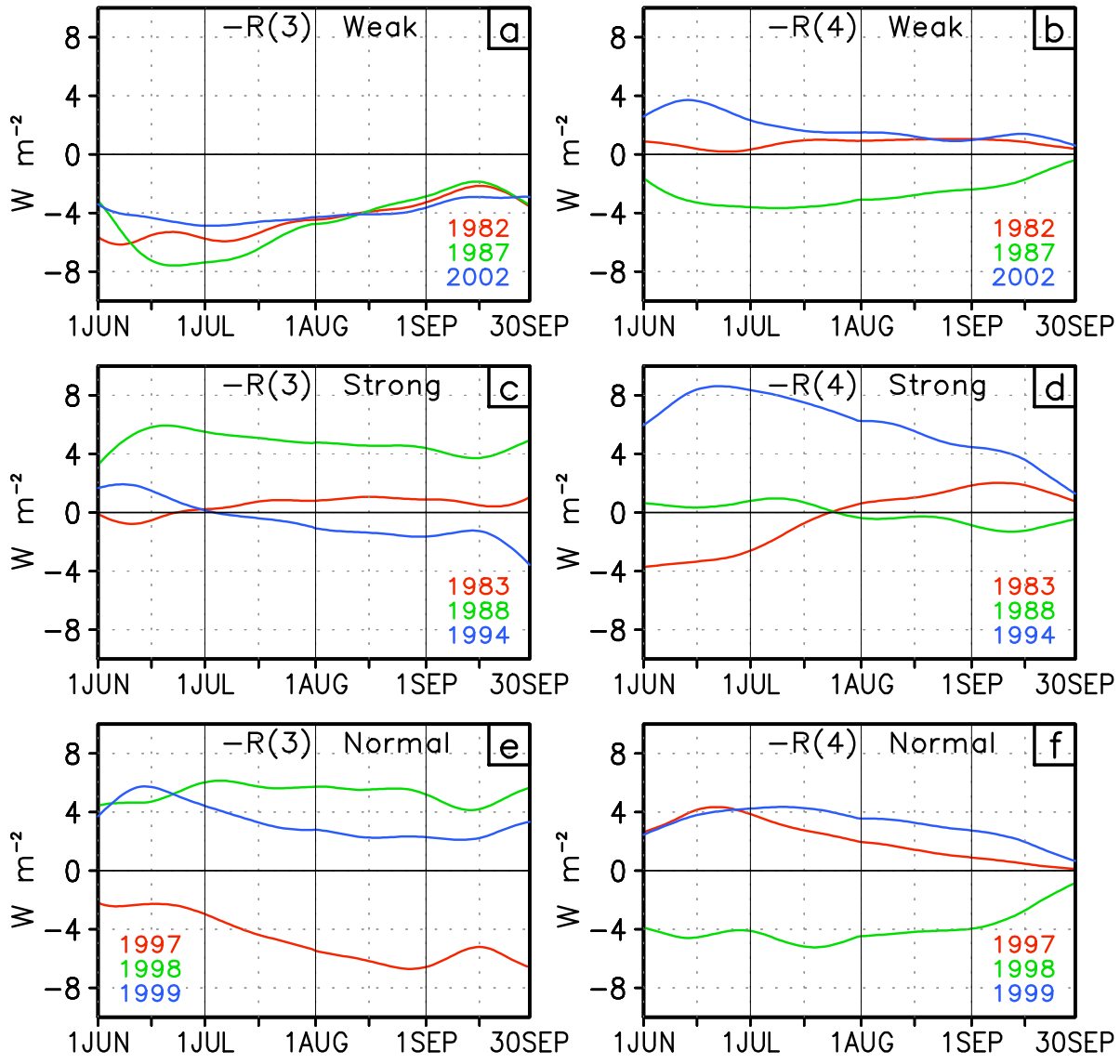

Fig. 15. Daily time series of $R(3)$ (left panels) and $R(4)$ (right panels) area averaged over the IMR region for JJAS. $R(3)$ and $R(4)$ are plotted with opposite sign for easy comparison with the rainfall average over India. Top panels (a, b) show the time series for three weak monsoon years and the middle panels (c, d) show three strong monsoon years. Bottom panels (e, f) show three years in 1990s when the rainfall over India is normal. The years are indicated in each panel.